Article
Volume 3, Number 5
31 May 2002
10.1029/2001GC000217
ISSN: 1525-2027

Geochemistry Geophysics Geosystems G3
AN ELECTRONIC JOURNAL OF THE EARTH SCIENCES
PUBLISHED BY AGU AND THE GEOCHEMICAL SOCIETY

The pMELTS: A revision of MELTS for improved calculation of phase relations and major element partitioning related to partial melting of the mantle to 3 GPa

Mark S. Ghiorso
Department of Earth and Space Sciences, Box 351310, University of Washington, Seattle, Washington 98195, USA (ghiorso@u.washington.edu)

Marc M. Hirschmann
Department of Geology and Geophysics, University of Minnesota, 310 Pillsbury Drive SE, Minneapolis, Minnesota 55455, USA (Marc.M.Hirschmann-1.umn.edu)

Peter W. Reiners
Department of Geology and Geophysics, Yale University, P.O. Box 208109, New Haven, Connecticut 06520, USA (peter.reiners@yale.edu)

Victor C. Kress, III
Department of Earth and Space Sciences, Box 351310, University of Washington, Seattle, Washington 98195, USA (kress@u.washington.edu)

[1] We describe a newly calibrated model for the thermodynamic properties of magmatic silicate liquid. The new model, pMELTS, is based on MELTS [*Ghiorso and Sack*, 1995] but has a number of improvements aimed at increasing the accuracy of calculations of partial melting of spinel peridotite. The pMELTS algorithm uses models of the thermodynamic properties of minerals and the phase equilibrium algorithms of MELTS, but the model for silicate liquid differs from MELTS in the following ways: (1) The new algorithm is calibrated from an expanded set of mineral-liquid equilibrium constraints from 2439 experiments, 54% more than MELTS. (2) The new calibration includes mineral components not considered during calibration of MELTS and results in 11,394 individual mineral-liquid calibration constraints (110% more than MELTS). Of these, 4924 statements of equilibrium are from experiments conducted at elevated pressure (200% more than MELTS). (3) The pMELTS model employs an improved liquid equation of state based on a third-order Birch-Murnaghan equation, calibrated from high-pressure sink-float and shockwave experiments to 10 GPa. (4) The new model employs a revised set of end-member liquid components. The revised components were chosen to better span liquid composition-space. Thermodynamic properties of these components are optimized as part of the mineral-liquid calibration. Comparison of pMELTS to partial melting relations of spinel peridotite from experiments near 1 GPa indicates significant improvements relative to MELTS, but important outstanding problems remain. The pMELTS model accurately predicts oxide concentrations, including SiO_2, for liquids from partial melting of MM3 peridotite at 1 GPa from near the solidus up to ~25% melting. Compared to experiments, the greatest discrepancy is for MgO, for which the calculations are between 1 and 4% high. Temperatures required to achieve a given melt fraction match those of the experiments near the solidus but are ~60°C high over much of the spinel lherzolite melting interval at this pressure. Much of this discrepancy can probably be attributed to overstabilization of clinopyroxene in pMELTS under these conditions. Comparison of pMELTS calculations to the crystallization and partial melting experiments of *Falloon et al.* [1999] shows excellent agreement but also suffers from exaggerated calculated stability of clinopyroxene. Finally, comparison of pMELTS

calculations to the garnet peridotite experiments of *Walter* [1998] at 3–7 GPa reveals disparities between calculations and experiments that increase with pressure. The most prominent of these disparities is manifest as overprediction of the stability of garnet and underprediction of that of olivine. Part of this problem may be attributed to inadequacies in the Birch-Murnaghan equation of state in reproducing the behavior of highly compressible liquids at high pressures and temperatures.

Components: 15,373 words, 16 figures, 7 tables.

Keywords: Mantle; partial melting; thermodynamic model; pMELTS; peridotite.

Index Terms: 3939 Mineral Physics: Physical thermodynamics; 3630 Mineralogy and Petrology: Experimental mineralogy and petrology; 3640 Mineralogy and Petrology: Igneous petrology; 3655 Mineralogy and Petrology: Major element composition.

Received 20 August 2001; **Revised** 14 January 2002; **Accepted** 21 January 2002; **Published** 31 May 2002.

Ghiorso, M. S., M. M. Hirschmann, P. W. Reiners, V. C. Kress III, The pMELTS: A revision of MELTS for improved calculation of phase relations and major element partitioning related to partial melting of the mantle to 3 GPa, *Geochem. Geophys. Geosyst.*, *3*(5), 10.1029/2001GC000217, 2002.

Theme: Geochemical Earth Reference Model (GERM) **Guest Editor:** Hubert Staudigel

1. Introduction

[2] Partial melting of the mantle has been studied using many tools, including those of analytical geochemistry, observational geophysics, experimentation, and application of physical and chemical theory. Through combination of these tools, substantial progress has been made in illuminating partial melting processes and basalt generation, particularly beneath mid-ocean ridges. One of the newer tools used to study these processes is MELTS, which applies thermodynamic models of minerals and silicate liquid to calculate phase equilibria as a function of intensive variables and bulk composition [*Ghiorso and Sack*, 1995]. For a full description of the MELTS computational algorithm, constituent thermochemical models and considerations of application to partial melting problems, see *Ghiorso and Sack* [1995] and *Hirschmann et al.* [1998b].

[3] Major topics addressed with earlier versions of MELTS include (1) the composition of near-solidus partial melts of peridotite [*Baker et al.*, 1995; *Hirschmann et al.*, 1998b, 1999a], (2) the production of melt during adiabatic upwelling [*Asimow et al.*, 1995, 1997, 2001; *Hirschmann et al.*, 1999b], (3) the effect of melt-rock reaction on melt and residual peridotite composition and the origin of dunites [*Asimow and Stolper*, 1999; *Kelemen and Dick*, 1995], (4) the effect of addition of water to hot peridotite on melting [*Eiler et al.*, 2000; *Hirschmann et al.*, 1999b] and (5) the relationship between mantle heterogeneity and melt composition [*Hirschmann et al.*, 1998b, 1999a; *Schiano et al.*, 2000]. These studies have demonstrated the unique value of the thermochemical modeling approach in exploring processes that cannot be reproduced with experiments or described with simple parametarizations. Insights gained from these efforts have changed the way we look at mantle melting and have inspired new avenues for experimental investigation.

[4] Despite these successes and prospects, application of MELTS to mantle melting has been limited by a number of critical problems. Predicted compositions of partial melts of peridotite are systematically displaced from experimentally determined compositions and the relationship between temperature and melt fraction is offset by ~100°C relative to experimental results [*Baker et al.*, 1995; *Hirschmann et al.*, 1998b]. Also, although the effect of water on solid-liquid phase relations is incorporated into MELTS, the adopted equation of state for water fails above 1 GPa. Several less prominent

imperfections are also present, as discussed in detail by *Hirschmann et al.* [1998b]. These deficiencies have limited the value of MELTS as a quantitative, as opposed to qualitative tool for exploring the consequences of partial melting during adiabatic upwelling.

[5] In this contribution we outline a number of refinements to the thermodynamic model for the silicate liquids incorporated in MELTS that render an improved ability to calculate phase equilibria related to partial melting of the shallow mantle. This revised model is packaged into a computational algorithm with equivalent functionally to MELTS that we will term pMELTS (the "p" stands for pressure).

1.1. Overview of the Problem

[6] From afar, recalibration of MELTS to better predict partial melting of peridotite and related lithologies may seem like a simple matter. One may seek to reproduce a selected set of relevant existing experiments on partial melting of peridotite by using those experiments as calibrates. However, a number of considerations prevent such a simple solution from being effective. The objections are both practical and philosophical.

[7] From a practical perspective, there are simply not enough experimental constraints of sufficient quality on mantle bulk compositions over the temperature (T), pressure (P) range of interest to calibrate a set of thermodynamic models that adequately describe phase equilibria in this system. Because of the complex nature of igneous phases, the underlying thermodynamic models used to describe them necessarily contain too many adjustable parameters to be unambiguously fitted to the limited existing experimental data set. This problem is compounded by the important factor that it is not possible to acquire an experimental data set where T, P, and phase composition are uncorrelated. Systematic shifts in mineral and liquid compositions with T and P substantially inhibit isolation of compositional variables from intensive variables. This situation exacerbates the tendency for model parameters calibrated from such a restricted data set to be correlated and for the resulting model (thermodynamic or otherwise) to be unsuitable for extrapolation beyond the domain-space of the set. In addition, the complexity of performing experiments at high pressure, the difficulty of characterizing the intensive variables of the experiments, and systematic interlaboratory discrepancies in experimental results render our knowledge of the phase-equilibrium relations involved in mantle melting at best incomplete and at times contradictory. Systematic interlaboratory errors in unrelated experimental studies can generate fictitious geochemical trends that are difficult to recognize and eliminate during the fitting process.

[8] Aside from the practical issues that prohibit calibrating a thermodynamic model of mantle melting solely from experiments on partial melting of peridotite and related lithologies, there is the underlying philosophical issue that motivates work on MELTS and its descendents. Thermodynamic models are useful and worth constructing because they provide a framework for extrapolating experimental results beyond the direct objectives of the experiments. If one is only interested in interpolating, smoothing, or systematizing experimental observations, then the best method to use is cubic splines [*Press et al.*, 1992]; the advantages gained in fitting observations to a thermodynamic formalism do not outweigh the difficulties and inconvenience if interpolation is all that is to be done with the model. In practice, however, pragmatic limitations dictate that experiments almost always involve some simplification and abstraction of the natural process they are designed to explore. Therefore most comparisons of experiments to natural occurrences involve some degree of extrapolation. Furthermore, if we are interested in performing calculations that are of a completely different nature than the experimental results (e.g., predicting the proportion of liquid during adiabatic, polybaric melting when we have available experiments detailing coexisting phase compositions at various T and P), then a thermodynamic formalism is worth the trouble.

[9] Such an ability to extrapolate comes at a cost. The underlying thermodynamic models for the solid and liquid phases that constitute the system must be complex enough to adequately characterize the energetics of these phases over a compositional, T and P range that generally far exceeds that of the

experiments. The models must be internally consistent, follow the rules of thermodynamics derived from the first and second laws, and consequently satisfy experimental constraints in addition to those foremost of interest (e.g., calorimetric constraints on reference state properties). The consequence for a computational thermodynamics package like MELTS (or pMELTS) is that the experimental database of phase equilibria used to calibrate the underlying thermodynamic models must have as broad a range of bulk compositions and intensive variables as is feasible. Our philosophy [*Ghiorso and Carmichael*, 1980; *Ghiorso*, 1983; *Hirschmann and Ghiorso*, 1994; *Ghiorso and Sack*, 1995] has been to use experimental data of liquid-solid phase equilibria on bulk compositions that span the entire range of silicate magma types found in nature and to reference model calibration to an internally consistent compilation of reference state properties of minerals [*Berman*, 1988]. Our specific goal in this paper is to improve the ability of MELTS to predict mantle phase-equilibria. We will proceed by refining the underlying thermodynamic models to achieve this objective, but we will not do so by excluding experimental data on other systems. Our goal is to make pMELTS a superset not a subset of MELTS.

1.2. Brief Thermodynamic Background

[10] MELTS uses methods of computational thermodynamics and thermodynamic models of minerals and melts to compute an equilibrium assemblage as a function of composition and T, P, or other intensive thermodynamic variable [*Ghiorso*, 1997]. The thermodynamic underpinnings of MELTS and their relevance to modeling partial melting of the mantle have been extensively discussed and reviewed in a number of previous papers [*Ghiorso et al.*, 1983; *Ghiorso and Sack*, 1995; *Hirschmann et al.*, 1998b]. Here we briefly review the salient characteristics of MELTS that are relevant to the revisions of the model presented in this work. The thermodynamic models for minerals used in pMELTS are the same as those used in MELTS [*Ghiorso and Sack*, 1995] and therefore will not be reviewed here. Differences between pMELTS and MELTS are the result of (1) revisions of the thermodynamic model for the silicate liquid, (2) adoption of a new reference model for H_2O, and (3) adoption of the Birch-Murnaghan volume equation of state.

[11] In MELTS and pMELTS, the molar Gibbs free energy of formation of silicate liquids is given by the function

$$\overline{G} = \sum_i X_i \mu_i^o - T\overline{S}^{\text{conf}} + \frac{1}{2}\sum_i \sum_j W_{ij} X_i X_j + RT[X_{H_2O} \ln X_{H_2O} + (1 - X_{H_2O}) \ln (1 - X_{H_2O})], \quad (1)$$

where μ_i^o is the standard state chemical potentials of a set of linearly independent compositional end-members and X_i are their mole fractions (X_{H_2O} refers specifically to water), $\overline{S}^{\text{conf}}$ is the molar configurational entropy,

$$\overline{S}^{\text{conf}} = -R\sum_i X_i \ln X_i - R\left[X_{H_2O} \ln X_{H_2O} + (1 - X_{H_2O}) \ln (1 - X_{H_2O})\right], \quad (2)$$

arising from a set of chemical species taken to be equivalent to thermodynamic components, and W_{ij} are a set of adjustable parameters (taken to be independent of T and P) that account for the nonideal contributions to mixing as inferred from experimentally determined compositions of silicate liquids and coexisting solids. Contributions to $\overline{G}$ as a function of T, P, and composition in pMELTS differs from that of MELTS in the following ways: (1) some standard state properties of liquid components (in particular the reference state enthalpy and entropy) are optimized during model calibration, whereas in MELTS these quantities are not adjusted. (2) The P dependence of μ_i^o is modeled using a third-order Birch-Murnaghan equation of state (EOS). (3) Definitions of thermodynamic components are modified, resulting in a different $\overline{S}^{\text{conf}}$ and. (4) The W_{ij} have been refit using an expanded database of experimental statements of mineral-liquid equilibria and a modified methodology. The details of these differences are described in the section 2.

2. New Model Features

2.1. Database Compilation

[12] MELTS is calibrated from an experimental database of liquid-solid equilibria compiled in

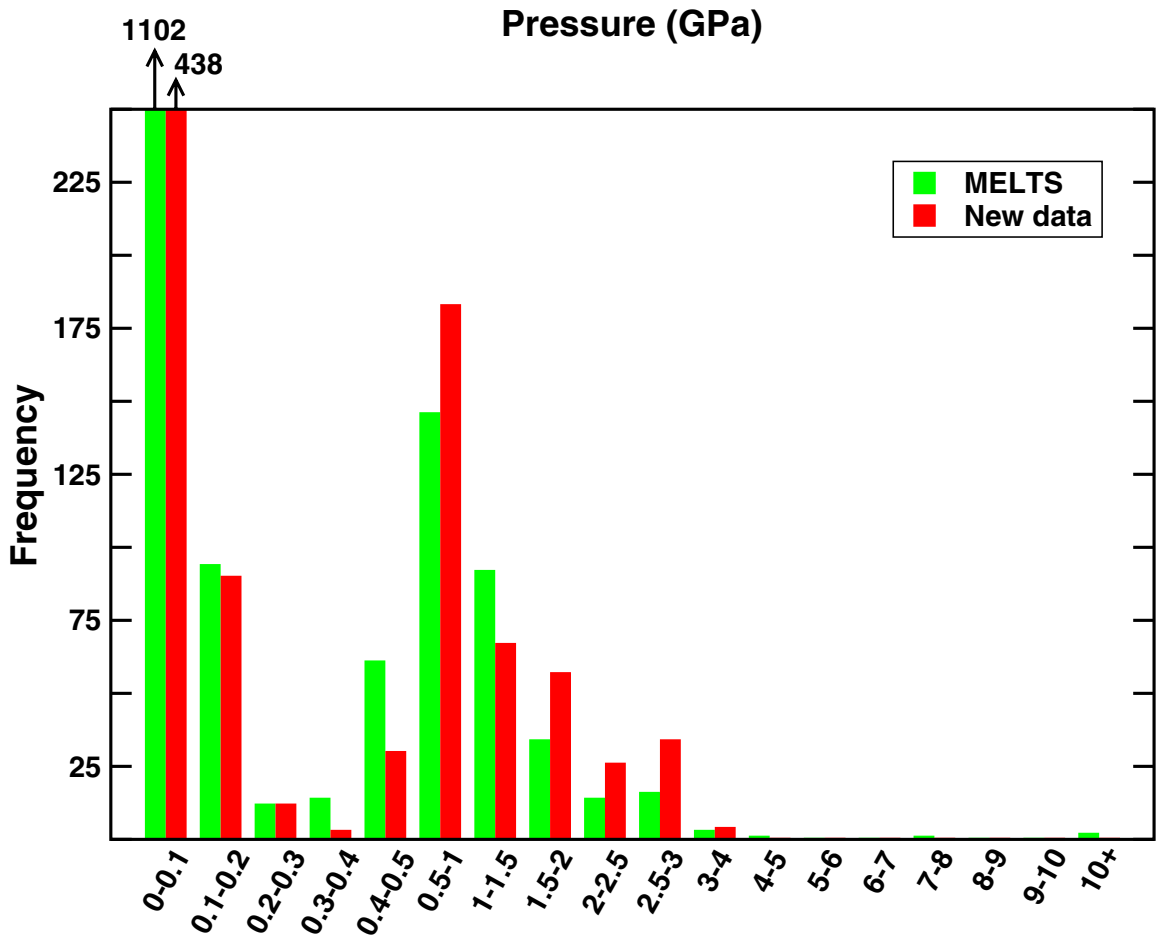

Figure 1. Pressure frequency histogram of experiments contained in the calibration database for pMELTS. Experiments included in original MELTS calibration [*Ghiorso and Sack*, 1995] are indicated by the green fill. Note that the ordinate is truncated and that true column heights are labeled for the lowest pressure grouping.

1992, and considerable new data have been published since that time. The original database comprised 1593 experiments that yielded 5433 statements of mineral-melt equilibria, including 1644 at $P > 10^5$ Pa. Given the predominance of low-pressure data in the original compilation, incorporation of new high-pressure data is of central importance to calibration of pMELTS. In appendix A we list the sources for a revised compilation. These new sources include material published after 1992 as well as some experiments published prior to 1992 but overlooked in the original compilation. The new database has 2439 experiments which yield 11,394 phase equilibrium constraints, including 4924 at $P > 10^5$ Pa. It should be noted that the size of a calibration database is not the only feature to examine when evaluating the quality of the phase equilibrium data used to constrain a MELTS-like model. Wide coverage of composition-temperature-pressure space is also an important feature (Figures 1 and 2).

[13] One consideration in compilation of a database of experimental phase equilibria for the purposes of calibrating thermodynamic models is the accuracy of reported physical and chemical conditions prevailing in solid media pressure (piston cylinder and multianvil) devices. Compared to experiments at one atmosphere or to some in gas media apparatuses, the T, P, and volatile fugacities of solid media experiments are less precisely and less accurately known. For example, standard uncertainties in T and P of piston cylinder measurements are ±10°C and 0.1 GPa, though in some cases actual uncertainties

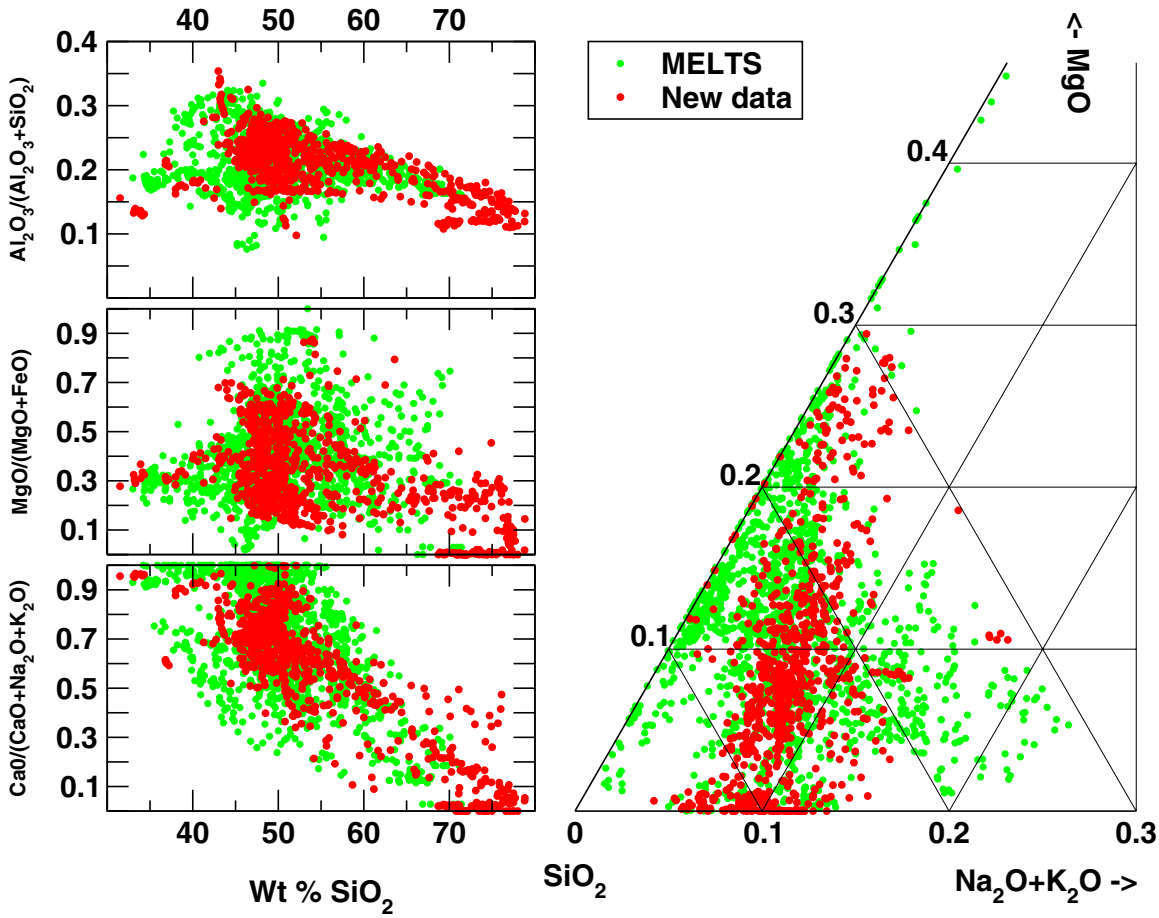

Figure 2. Compositional variation of experimental liquids contained in the calibration database for pMELTS. Experiments included in original MELTS calibration [*Ghiorso and Sack*, 1995] are indicated by green circles. Units are wt %.

can be significantly larger [*Hirschmann*, 2000; *Longhi*, 1998]. For multianvil experiments, pressure uncertainties are of the order of 0.5 GPa [*Luth*, 1993], and uncertainties in temperature, though not well characterized, can easily be several tens of degrees, owing to large temperature gradients [e.g., *Herzberg and Zhang*, 1997; *Walter et al.*, 1995].

[14] The effect on thermodynamic calibrations of imperfect characterization of intensive variables during solid media experiments can be significant. For example, the chemical potential of a liquid component defined by a mineral-liquid reaction such as

$$\underset{\text{forsterite}}{Mg_2SiO_4} \Leftrightarrow \underset{\text{liquid}}{Mg_2SiO_4}$$

varies by ~500 J if the temperature is 10°C different from the published value. The effect of 0.1 GPa pressure uncertainty is ~100 J. Even larger errors are suggested when one compares experimental determinations of a given mineral-liquid reaction by several laboratories. These errors are typically of the order of ~3–5 kJ [*Ghiorso et al.*, 1983; *Ghiorso and Sack*, 1995, this work]. *T*, *P* uncertainties can have a significant deleterious effect on the quality of the liquid model if they are systematic rather than random. For example, they may strongly affect the accuracy of the liquid model if temperatures or pressures are systematically high or low for a set of experiments that cover a range of liquid compositions that are not otherwise well represented in the calibration database.

[15] A potentially pernicious problem in application of high-pressure experiments to thermodynamic model calibration is the presence of uncharacterized

quantities of volatiles such as H_2O and CO_2. H_2O is a common contaminant in nominally anhydrous experiments. For example, *Hirschmann et al.* [1998a] documented 0.4 wt % H_2O in experimentally produced nominally anhydrous low degree partial melts of peridotite reported originally by *Baker et al.* [1995]. Unfortunately, the amount of water present in glasses produced in solid media apparatus experiments depends on assembly material, the drying procedure for the assembly and the sample powder, the duration of the experiment, and the proportion of phases with nonnegligible volatile solubility present in the experimental charge. Consequently, there is no accurate and universal method for correcting for the amount of water if the liquids are not characterized. Similarly, liquids from experiments conducted in graphite capsules generally contain a small quantity of dissolved CO_2. Graphite-saturated basaltic liquids have ~0.2 wt % CO_2 at 1 GPa [*Holloway*, 1998] and, in some cases, CO_2 can invade charges by diffusion through noble metal capsules; for example, *Gaetani and Grove* [1998] found up to 1.3 wt % CO_2 in hydrous melt-mineral experiments in which graphite was located outside AuPd capsules. To a lesser extent, some solid media assemblies may also introduce small amounts of chlorine, fluorine, and/or boron. Relatively modest quantities of volatiles in nominally volatile-free experiments can have a significant effect on the temperature-composition location of mineral cotectics and, if unaccounted for, can result in significant error in constraints placed by mineral-melt experiments on liquid thermodynamic properties.

[16] An additional variable that is typically unconstrained in solid-media apparatus experiments is the ratio of ferric iron to ferrous iron in silicate liquids and coexisting solid solutions. Unlike in one atmosphere experiments, where a known oxygen fugacity normally allows precise estimation of the liquid ferric/ferrous ratio [e.g., *Kress and Carmichael*, 1991], the oxygen fugacity is not well known in many solid media experiments. Therefore the speciation of FeO and Fe_2O_3 in silicate liquids and coexisting solid solutions in these experiments is often poorly constrained. For experiments conducted in graphite capsules, most iron in the melt is likely to be ferrous, and we calculate Fe_2O_3 and FeO in these silicate liquids by assuming that oxygen fugacity conforms to the C-CO-CO_2 buffer [*Huebner*, 1971]. This likely represents a small overestimate of the ferric iron present.

2.2. Modified Set of Standard State Components

[17] The thermodynamic model for the liquid phase adopted in MELTS and pMELTS and embodied in equations (1) and (2) is a highly simplified description of melt energetics in terms of molecular mixing of a set of hypothetical end-member components. These hypothetical thermodynamic components are proxies for actual melt species, which is at best a crude assumption. The inadequacy of this assumption limits the applicability of the resulting model to natural-composition liquids. Nonideal contributions to the energy of mixing are accounted with simple regular-solution like pairwise interaction energy terms between these melt species.

[18] *Ghiorso and Sack* [1995] chose liquid component stoichiometries for MELTS that correspond to "mineral-like" molecules. This was done largely for convenience of calculation of end-member properties and to allow MELTS to span a wide range of liquid compositions. It was not realized at the time, however, that application of this component set to natural composition liquids caused the spectrum of liquid composition (expressed as mole% of the liquid species) to be highly skewed toward high mole fractions of silica. This can be visualized in Figure 3, where we have plotted the liquid compositions from the liquid-solid experimental database discussed above in terms of mole% of end-member components adopted for MELTS. Notice that the mole fractions of SiO_2 are quite high compared to the mole fractions of other liquid components whose population centroids lie at roughly 10 mole%. Although there is nothing wrong in theory with this skewed scatter of liquid compositions (and the success of MELTS upholds this), it does present the following difficulty. The free parameters of the liquid thermodynamic model that are used to account for nonideality and are fitted from the liquid-solid

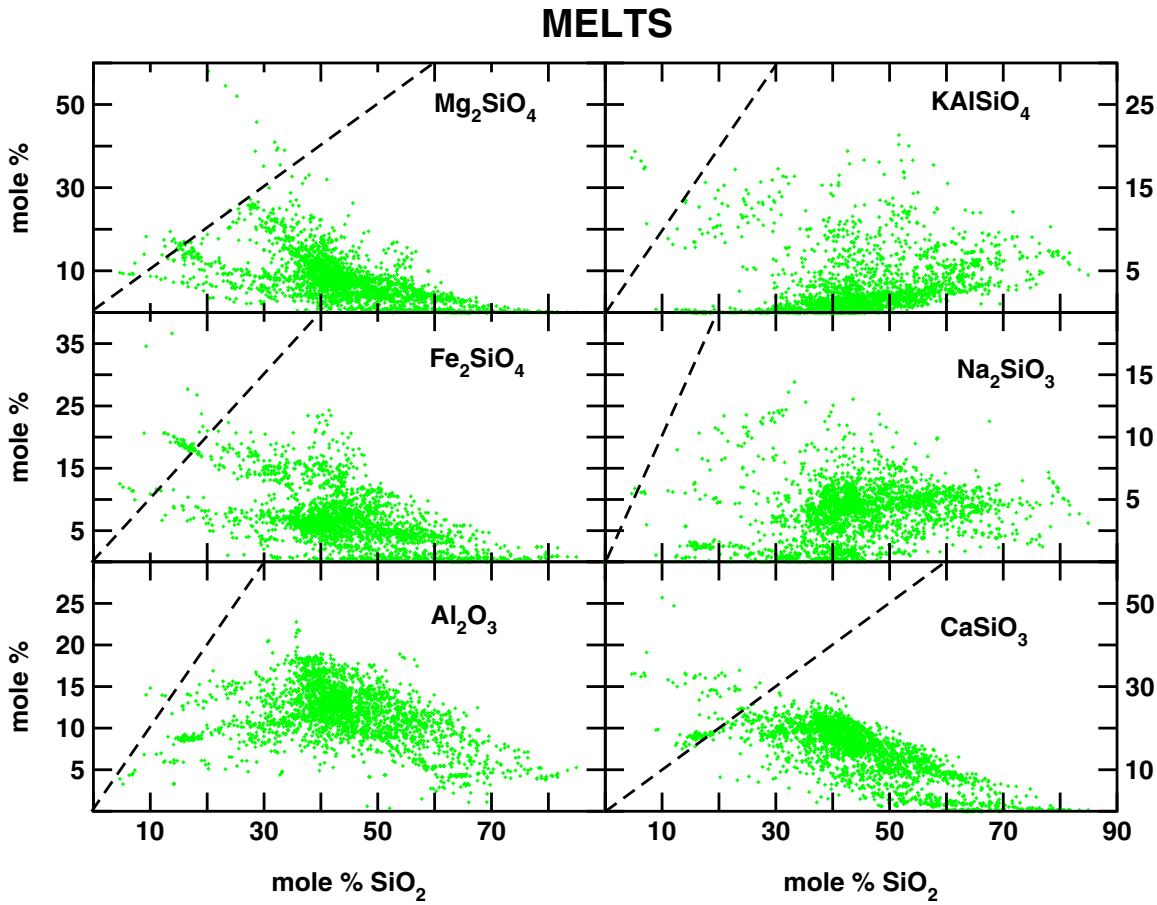

Figure 3. Concentration (in mole %) of liquid thermodynamic components defined in MELTS [*Ghiorso and Sack*, 1995] plotted against mole % of SiO_2 in the liquid for experimental liquids contained in the calibration database. Dashed lines give a reference for equal concentrations.

phase equilibria in the experimental database [*Ghiorso and Sack*, 1995] enter into the expression for the Gibbs energy of the system as quadratic products of species mole fractions (equation (1)). The ability for a particular W_{ij} term to influence the Gibbs energy is therefore proportional to the magnitude of the associated mole fraction product. With a skewed distribution of liquid compositions, most of these mole fraction products are small, and variation in these small products, even if large in relative proportion, are not given due weight by the numerical procedures utilized to fit the model to the database. In effect, fewer model parameters are operative simply because the input data are not evenly distributed over the parameter-space domain. Additionally, this skewed distribution minimizes the influence of the configurational entropy term (equation (2)) because maximal values of $\overline{S}^{\mathrm{conf}}$ are achieved at the midpoint composition and the contribution becomes nil at the vertices of composition-space.

[19] To remedy this situation, we constructed pMELTS by the method of *Barron* [1981] in which the stoichiometry of end-member liquid components in the model is adjusted. We make these adjustments so that the centroid of compositions in the experimental database comes closer to the midpoint of the feasible space (therefore maximizing the importance of the entropy term) and so that the average value of individual component mole fractions of major constituents is approximately the same. Trial and error gives the set of adopted liquid components for pMELTS. Changes from the

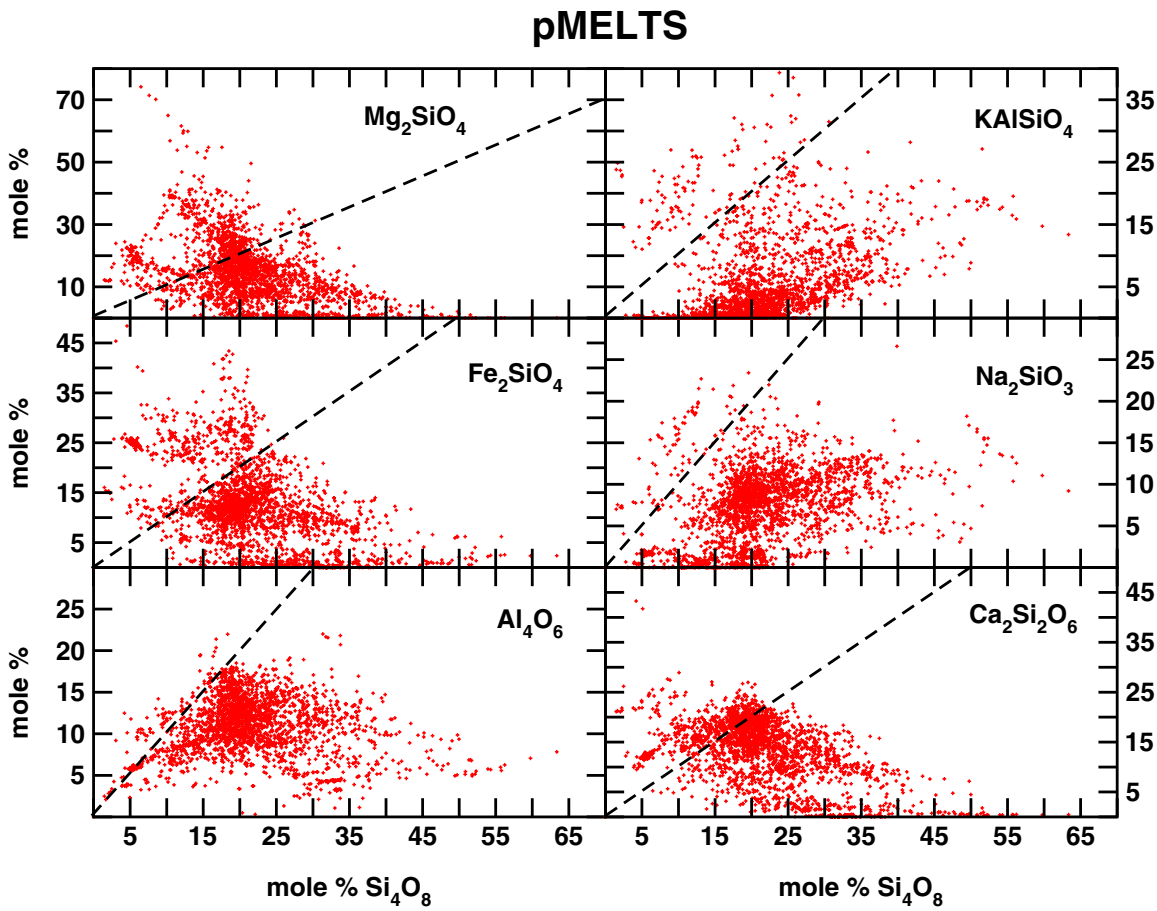

Figure 4. Concentration (in mole %) of liquid thermodynamic components defined in this paper for pMELTS plotted against mole % of Si_4O_8 in the liquid for experimental liquids contained in the calibration database. Dashed lines give a reference for equal concentrations.

MELTS set include $SiO_2 \rightarrow Si_4O_8$, $Al_2O_3 \rightarrow Al_4O_6$, $CaSiO_3 \rightarrow Ca_2Si_2O_6$, and $Na_2SiO_3 \rightarrow NaSi_{0.5}O_{1.5}$; the most important change in stoichiometry being that of the silica component. In Figure 4 we illustrate component mole fractions for liquid in the experimental database plotted in terms of pMELTS components.

2.3. Fitting Standard State Properties

[20] In the thermodynamic model for silicate liquid contained in MELTS, the standard state is taken to be unit activity of the pure liquid component at any T and P. The standard state properties of the liquid are calculated from corresponding values for solid phases of matching stoichiomentry [*Berman*, 1988] converted to the liquid phase using measured or estimated enthalpies of fusion (see Appendix B). They are not adjustable parameters in the MELTS fit.

[21] In pMELTS we adopt the modified standard state definition of unit activity of a hypothetical liquid, referenced to a multicomponent silicate melt of the specified composition range of naturally occurring liquids, at unit mole fraction and any T and P. This means that the standard state includes any "melt structure" modifications that arise in passing from the pure liquid to that of a multicomponent melt. For example, it is generally accepted that Al in Al_2O_3 liquid is sixfold coordinated. If, as in MELTS, Al_2O_3 is chosen as a liquid component and its properties are computed from the fusion of corundum, then implicitly the Al_2O_3 liquid component has the energetics of sixfold coordinated aluminum. If these Al_2O_3 liquid prop-

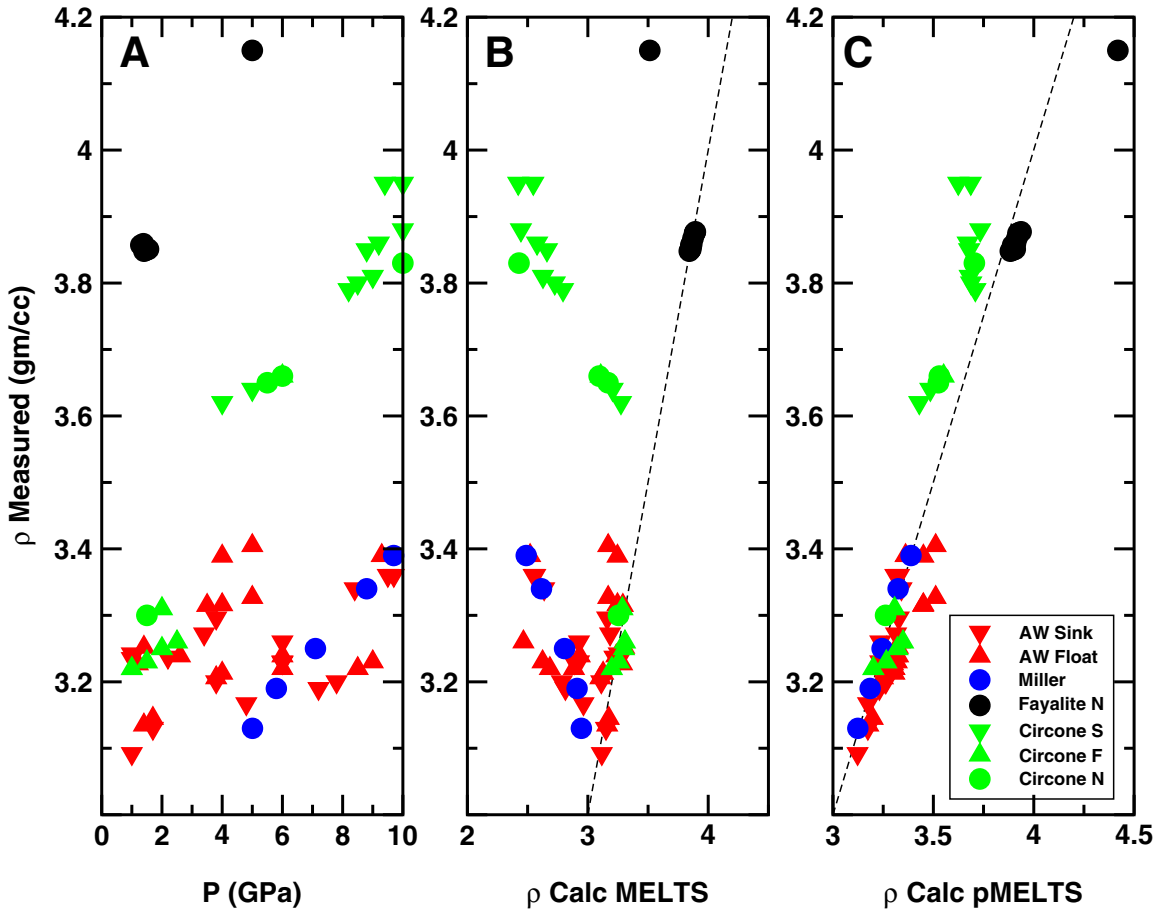

Figure 5. High-pressure density estimates used to calibrate the liquid EOS for pMELTS. (a) Density determinations plotted versus pressure. (b) Density determinations plotted versus estimates computed from the MELTS EOS [*Ghiorso and Sack*, 1995]. (c) Density determinations plotted versus estimates computed from the pMELTS EOS (this paper, K' = 5). Sources of data are as follows: AW [*Agee and Walker*, 1990, 1993], Miller [*Miller*, 1991], Fayalite [*Agee*, 1992a, 1992b], Circone [*Circone and Agee*, 1996]; S, sink; F, float; N, neutral bouyancy.

erties are applied to multicomponent silicate liquids at low pressure, the energetic consequences of the change in coordination state of Al from sixfold to fourfold must then be absorbed into the excess Gibbs energy of mixing. This is what is done in MELTS, but in pMELTS the pure Al_2O_3-liquid thermodynamic properties are adjusted to create a hypothetical fourfold coordinated Al_2O_3-liquid. The disadvantage of the pMELTS liquid standard state choice is that the adopted properties of the pure components depend on both the calibration database and upon the form of the mixing model for the property of interest. In the pMELTS calibration we have chosen to adjust values of the enthalpy and entropy of selected liquid end-member properties to accommodate melt structure changes between the pure liquid and the multicomponent liquids of interest.

2.4. Modified Equation of State (EOS) of Silicate Liquid

[22] When the silicate liquid thermodynamic model that forms the core of MELTS was formulated in the early 1990s, extrapolation of phase equilibria to mantle pressures was not an anticipated application. Consequently, a very simple EOS,

$$V = a + b(T - T_r) + c(P - P_r) + d(T - T_r)(P - P_r) + e(P - P_r)^2, \quad (3)$$

was utilized for the liquid phase, with constants *a, b, c*, and *d* taken from the work of *Lange and*

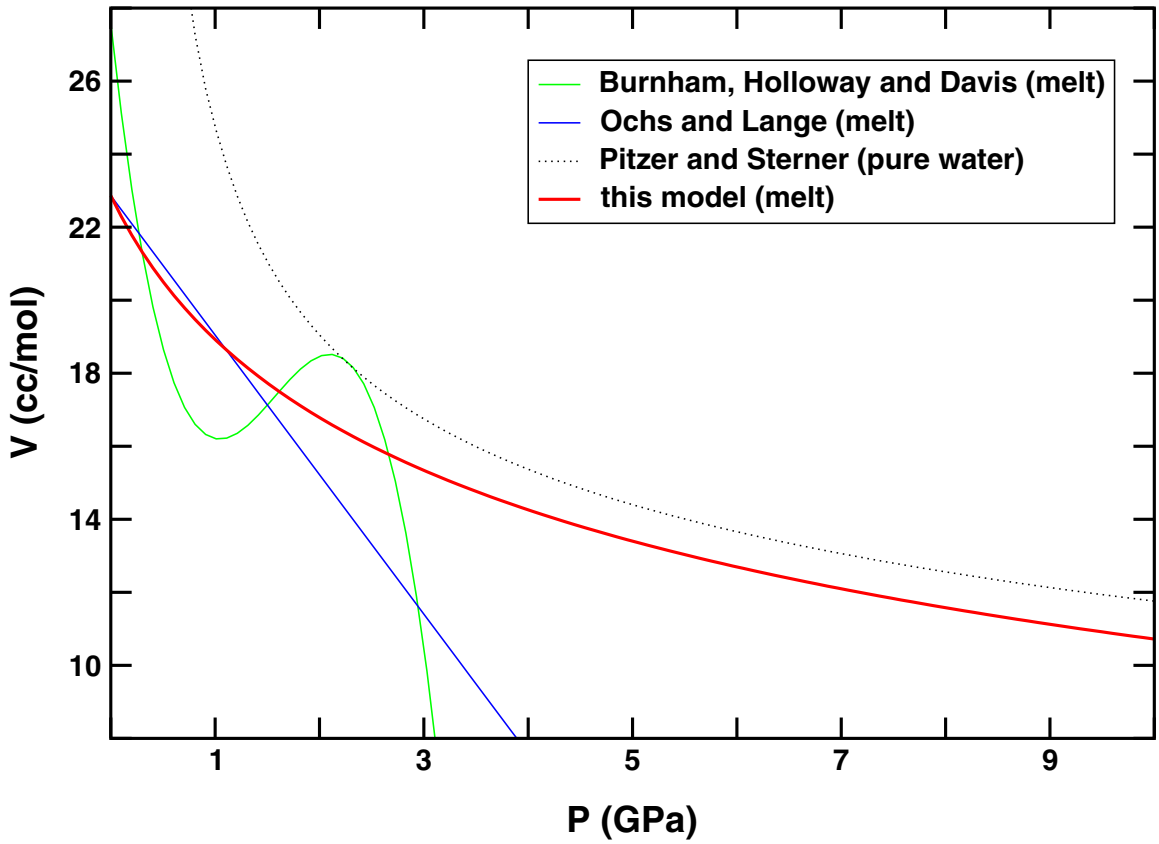

Figure 6. Analysis of EOS behavior for dissolved H_2O in silicate melts and for pure H_2O fluid (dotted line, [*Pitzer*, 1994]). Green line is the original model EOS of *Burnham et al.* [1969]. Blue straight line is the proposed EOS of *Ochs and Lange* [1997]. Red curve is the EOS adopted in this study. In contrast to the functions of *Burnham et al.* [1969] and *Ochs and Lange* [1997], the EOS adopted in this study yields properties of H_2O in silicate liquids that remain similar to those of pure H_2O up to high pressure.

Carmichael [1990] and *Kress and Carmichael* [1991]. The constant, e, was estimated from fusion curve analysis [*Ghiorso and Sack*, 1995]. Application of MELTS to mantle melting demonstrates that this approximation is inadequate above 2 GPa. We have replaced this simple EOS with a third-order Birch-Murnaghan equation,

$$P = \frac{3}{2}K\left[\left(\frac{V_o}{V}\right)^{\frac{7}{3}} - \left(\frac{V_o}{V}\right)^{\frac{5}{3}}\right]\left\{1 - \frac{3}{4}(4 - K')\left[\left(\frac{V_o}{V}\right)^{\frac{2}{3}} - 1\right]\right\}, \quad (4)$$

taking values of V_0 and K (for all melt components excluding water, see section 2.5) from *Lange and Carmichael* [1990] and *Kress and Carmichael* [1991], and constraining a value for K'; (see Figure 5) from olivine sink-float experiments of *Agee and Walker* [1988,1993] and shock wave experiments of *Miller et al.* [1991]. The new formulation affords extrapolation of liquid properties to ~4 GPa and is incorporated in the pMELTS calibration described in section 3. Methods of calculating molar Gibbs free energies of end-member components are discussed in Appendix B.

2.5. Revised Properties of H_2O in Silicate Liquid

[23] In MELTS, the solubility of water and the influence of dissolved water on solid-liquid phase equilibria are described by a thermodynamic model for dissolved H_2O and another for the pure fluid phase. *Ghiorso and Sack* [1995] chose to base their calibration on the *Burnham et al.* [1969] EOS for dissolved H_2O in the melt and the *Haar et al.* [1984] formulation for liquid water, which though highly accurate and internally consistent with other

mineral thermodynamic properties [*Berman*, 1988], is valid only below 1 GPa. At the time MELTS was calibrated, it was surmised that the Burnham EOS was likely restricted to pressures below 1 GPa but confirming experimental results, even at low pressure, were lacking. As shown in Figure 6, the *Burnham et al.* [1969] EOS extrapolates poorly to elevated pressures.

[24] In pMELTS, we adopt the EOS for pure water of *Pitzer and Sterner* [1994]. Although it is slightly less accurate than the equation of *Haar et al.* [1984], it is valid to pressures up to 10 GPa and is more convenient to utilize than other alternative EOSs over this extended pressure range.

[25] For the thermodynamic properties of water dissolved in the silicate melt, we have utilized the new measurements (and revised calibration of *Burnham et al.* [1969]) provided by *Ochs and Lange* [1997]. *Ochs and Lange* [1997] give reference state properties of H_2O dissolved in silicate melt in the form of a simple EOS that is meant to be applied at pressures up to 1 GPa:

$$V^o_{H_2O} = V^o_{H_2O,T_r,P_r} + \left.\frac{\partial V^o_{H_2O}}{\partial T}\right|_{T_r,P_r}(T - T_r) + \left.\frac{\partial V^o_{H_2O}}{\partial P}\right|_{T_r,P_r}(P - P_r). \quad (5)$$

When extrapolated to pressures substantially greater than 1 GPa, (5) results in an unrealistically low partial molar volume of H_2O (Figure 6). Consequently, we have chosen to recast the *Ochs and Lange* [1997] results into a form compatible with the Birch-Murnaghan equation. We take the reference volume and its temperature derivative ($V^o_{H_2O,T_r,P_r}$, $\left.\frac{\partial V^o_{H_2O}}{\partial T}\right|_{T_r,P_r}$, $T_r = 1673$ K, $P_r = 10^5$ Pa) from *Ochs and Lange* [1997], and adjust a value of K and K'; in the Birch-Murnaghan equation (e.g., equation (4)) to (1) exactly match the result from equation (5) at 1 GPa and (2) match the compressibility of pure H_2O liquid computed from the EOS of *Pitzer and Sterner* [1994] at elevated pressure (see Figure 6). This analysis results in the model EOS plotted in Figure 6, a value of K' of 3.5, and a revised value of $\left.\frac{\partial V^o_{H_2O}}{\partial P}\right|_{T_r,P_r}$ of -6×10^{-15} m^3/mol-Pa. which should be compared to the value reported by *Ochs and Lange* [1997], $-3.82(\pm 0.36, 1\sigma) \times 10^{15}$ m^3/mol-Pa.

2.6. Extended Calibration Statements

[26] The method of calibrating liquid thermodynamic properties from solid-liquid equilibria in pMELTS is essentially that of MELTS [*Ghiorso and Sack*, 1995] with one additional feature. In pMELTS we have utilized statements of solid-liquid equilibria generated from "redundant" (i.e., linearly dependent) solid components. The best way to describe this is by example. Consider an experiment involving coexisting pyroxene and silicate melt at some T and P. In MELTS, statements of liquid-solid equilibrium would be written, one for each independent thermodynamic component in the pyroxene. Thus if the pyroxene had a composition in the quadrilateral, three calibration equations would be written corresponding to the quadrilateral pyroxene components chosen by *Sack and Ghiorso* [1994]: (1) $\mu^{pyx}_{CaMgSi_2O_6} = \mu^{liq}_{CaMgSi_2O_6}$, (2) $\mu^{pyx}_{CaFeSi_2O_6} = \mu^{liq}_{CaFeSi_2O_6}$, and (3) $\mu^{pyx}_{Mg_2Si_2O_6} = \mu^{liq}_{Mg_2Si_2O_6}$. In the model regression of liquid properties for pMELTS, we add a redundant regression equation: $\mu^{pyx}_{Fe_2Si_2O_6} = \mu^{liq}_{Fe_2Si_2O_6}$, which, because of the reciprocal solution nature of the pyroxene quadrilateral, is actually a linearly dependent combination of the previous three. The reason to add these redundant equations to the model calibration process is to increase the stability of the parameter inversion process and to insure Fe/Mg and other exchange K_D values are modeled properly for each phase. In practice, the important "dependent" solid component additions in pMELTS include $Fe_2Si_2O_6$ (ferrosilite), $MgAl_2SiO_6$ (Mg-Tschermaks), $FeAl_2SiO_6$ (Fe-Tschermaks), and $CaAl_2SiO_6$ (Ca-Tschermaks) in the pyroxenes and $MgCr_2O_4$ (picrochromite), $MgFe_2O_4$ (magnesioferrite), and Mg_2TiO_4 (qandilite) in the spinels.

3. Model Calibration

[27] The calibration database assembled for the pMELTS regression yields 11,394 solid-liquid phase equilibrium constraints on the chemical potentials of liquid components. These are distributed over the phases and end-member solid-solution components as listed in Table 1. Model calibration is accomplished using standard inversion techniques based upon singular value analysis

Table 1. Contributions to Regression Problem

Phase	Component	Abbreviation	% contribution
Olivine			21.45
	Fayalite	Fa	10.70
	Forsterite	Fo	10.75
Garnet			2.20
	Almadine	Alm	0.75
	Grossular	Grs	0.75
	Pyrope	Pyr	0.69
Orthopyroxene			7.46
	Diopside	ODi	1.70
	Enstatite	OEn	2.24
	Hedenbergite	OHd	1.52
	Ferrosilite	OFs	1.04
	Mg-Tschermaks	Mat	0.48
	Fe-Tschermaks	Fat	0.48
Clinopyroxene			32.11
	Diopside	CDi	10.77
	Enstatite	CEn	8.11
	Hedenbergite	CHd	8.34
	Ferrosilite	CFs	3.54
	Ca-Tschermaks	Cat	1.36
Feldspar			16.75
	Albite	Ab	8.11
	Anorthite	An	8.21
	Sanidine	Sn	0.44
Quartz		Qtz	0.35
Tridymite		Try	0.18
Nepheline			0.22
	Na-Nepheline	Ne	0.11
	K-Nepheline	KNe	0.11
Leucite		Lc	0.63
Corundum		Crn	0.01
Spinel			13.11
	Chromite	Chr	1.48
	Hercynite	Hrc	3.90
	Magnetite	Mag	1.66
	Spinel	Spn	3.19
	Ulvospinel	Ulv	1.66
	Mg-Chromite	MCh	0.79
	Mg-Ferrite	MFe	0.42
	Qandilite	Qdn	0.02
Rhombohedral Oxide			3.36
	Geikielite	Gk	1.35
	Hermatite	Hm	0.75
	Ilmenite	Il	1.26
Whitlockite		Wh	0.06
Apatite		Ap	0.01
Water		Wat	2.10

in order to minimize correlation of the extracted parameters. The rank of the inversion (Table 2) is estimated by trial and error, utilizing techniques outlined by *Lawson and Hanson* [1974]. Interaction parameters between the components Si_4O_8, TiO_2, Al_4O_6, Fe_2O_3, $MgCr_2O_4$, Fe_2SiO_4, Mg_2SiO_4, $Ca_2Si_2O_6$, $NaSi_{0.5}O_{1.5}$, $KAlSiO_4$, $Ca_3(PO_4)_2$, and H_2O were fitted to the model (Table 3). Additional parameters included adjustments to the standard state enthalpies of the same components and adjustments to the standard state entropies of Si_4O_8, Al_4O_6, Fe_2O_3, Fe_2SiO_4, Mg_2SiO_4, $Ca_2Si_2O_6$, and $KAlSiO_4$ (Table 4, with further details of adopted standard state properties of liquid components in Tables B1–B3). Selection of the latter was made by trial and error with the

Table 2. ANOVA Analysis of Solid-Liquid Regression Problem

	DF	Sum of Squares	Mean Square	*F*
Regression	82	7,204,050	87,854.3	6,138.12
Residuals	11,311	161,893	14.3129	
Total	11,393	7,365,943	646.532	

goal of minimizing the temperature dependence of model residuals both globally and for individual mineral-liquid pairs.

[28] The statistics of the model inversion (Table 2) indicate that the solution is rank deficient as expected [*Ghiorso et al.*, 1983], as there are significant correlations between liquid components in the calibration data. This makes it impossible to fix independent values for all of the interaction terms. These linear dependencies between components also mean that uncertainties cannot be assigned to individual model parameters. The number of independent parameters in the inversion is the calculated problem rank: 82 (Table 2). Because of the linear dependency in the parameter set, the values ascribed to these parameters should not be taken out of context of the liquid model presented here. These values are meaningful only in the context of the standard state properties adopted or derived for the end-member liquid components. In addition, the parameters are not applicable to simple chemical systems and should not be used for synthetic liquids with a set of compositional components that is reduced relative to that found in natural magmatic settings.

[29] The overall fit to residuals of ±3.770 kJ (1σ) is a measure of the average ability to recover the chemical potential of a solid component of a mineral phase utilized in the calibration. To provide a sense of the relationship between this value and the ability of the model to recover experimental saturation temperatures, it is instructive to consider the analysis of residuals displayed in Figure 7. In this figure each solid component end-member utilized in the calibration is plotted and the average residual for that component and standard deviation about that average is indicated by the ordinate position. As an example of how to interpret these numbers, take the forsterite component of olivine, which has an average residual of 0.226 (0.06 × 3.770) kJ and a standard deviation of residuals of 2.149 (0.57 × 3.770) kJ. These numbers can be translated to offsets in recovery of experimental temperatures by normalizing by the entropy of the end-member. Taking average values of *T* and *P* of 1200°C and 0.1 GPa, the entropy of forsterite is found to be 345.84 J/K-mol [*Berman*, 1988]. Therefore the forsterite liquid equilibria are recovered ±2149/345.84 ≈ ±6(1σ)°C, and the systematic offset in these residuals is +226/345.84 ≈ +0.7°C; the plus sign on the systematic offset should be interpreted as appearance of the phase at higher temperatures than that indicated experimentally.

[30] As can be seen from Figure 7, there is little systematic error to the fit for the end-member components of olivine, orthopyroxene, feldspar, and for most of the spinel components. The standard deviations of residuals for these minerals imply temperature uncertainties of the order of ±5°C. Notable exceptions are the pyrope and almandine components in garnet, which have average residuals of −3.808 (−1.01 × 3.770) kJ and −8.030 (−2.13 × 3.770) kJ, respectively. These numbers translate to systematic temperature offsets of −3808/519.17 ≈ −7°C for pyrope and −8030/522.89 ≈ −15°C for almandine (*T* and *P* taken to be 1200°C and 0.1 GPa, entropies calculated from *Berman* [1988]). Note that these temperature offsets are negative, which implies that garnet is too stable and that calculated garnet compositions will be too Fe-rich.

[31] Correlations of residuals to temperature and pressure are statistically insignificant, except at pressures greater than ∼3 GPa. This is explored in some detail below in section 4.3 discussing *Walter*'s [1998] garnet peridotite partial melting experiments. In practical terms, calculations involving pMELTS should be limited to pressures lower than ∼3GPa.

[32] The pMELTS calibration residuals represent a significant improvement over MELTS [*Ghiorso and Sack*, 1995], and this is especially true for experiments in the pressure range 1–2 GPa. The best way to see the advantages of pMELTS over MELTS is to compare predictions of phase equilibria against experimental results for a few data

Table 3. Model Parameter Values

Component	Component	*W*, J
TiO_2	Si_4O_8	15,094.7
Al_4O_6	Si_4O_8	−296,975.2
Fe_2O_3	Si_4O_8	−164,027.4
$MgCr_2O_4$	Si_4O_8	37,459.2
Fe_2SiO_4	Si_4O_8	−18,841.4,
Mg_2SiO_4	Si_4O_8	−33,833.5
$Ca_2Si_2O_6$	Si_4O_8	−34,232.9
$NaSi_{0.5}O_{1.5}$	Si_4O_8	−59,822.7
$KAlSiO_4$	Si_4O_8	−102,706.5
$Ca_3(PO_4)_2$	Si_4O_8	37,519.9
H_2O	Si_4O_8	−45,181.6
Al_4O_6	TiO_2	−144,804.9
Fe_2O_3	TiO_2	−212,292.3
$MgCr_2O_4$	TiO_2	−22,455.8
Fe_2SiO_4	TiO_2	9,324.2
Mg_2SiO_4	TiO_2	16,355.6
$Ca_2Si_2O_6$	TiO_2	−9,471.5
$NaSi_{0.5}O_{1.5}$	TiO_2	22,194.2
$KAlSiO_4$	TiO_2	−3,744.0
$Ca_3(PO_4)_2$	TiO_2	65,544.0
H_2O	TiO_2	70,663.0
Fe_2O_3	Al_4O_6	−393,566.0
$MgCr_2O_4$	Al_4O_6	−269,339.7
Fe_2SiO_4	Al_4O_6	−200,788.1
Mg_2SiO_4	Al_4O_6	−192,709.0
$Ca_2Si_2O_6$	Al_4O_6	−270,700.8
$NaSi_{0.5}O_{1.5}$	Al_4O_6	−205,068.6
$KAlSiO_4$	Al_4O_6	−114,506.5
$Ca_3(PO_4)_2$	Al_4O_6	−176,584.1
H_2O	Al_4O_6	−161,944.4
$MgCr_2O_4$	Fe_2O_3	201,536.3
Fe_2SiO_4	Fe_2O_3	−211,493.4
Mg_2SiO_4	Fe_2O_3	−196,914.9
$Ca_2Si_2O_6$	Fe_2O_3	−146,008.1
$NaSi_{0.5}O_{1.5}$	Fe_2O_3	−123,728.7
$KalSiO_4$	Fe_2O_3	−130,847.5
$Ca_3(PO_4)_2$	Fe_2O_3	−126,339.8
H_2O	Fe_2O_3	−114,508.6
Fe_2SiO_4	$MgCr_2O_4$	−74,759.0
Mg_2SiO_4	$MgCr_2O_4$	−3,638.5
$Ca_2Si_2O_6$	$MgCr_2O_4$	48,337.5
$NaSi_{0.5}O_{1.5}$	$MgCr_2O_4$	−43,302.5
$KAlSiO_4$	$MgCr_2O_4$	124,517.4
Fe_2SiO_4	$MgCr_2O_4$	−74,759.0
$Ca_3(PO_4)_2$	$MgCr_2O_4$	13,004.3
H_2O	$MgCr_2O_4$	−18.9
Mg_2SiO_4	Fe_2SiO_4	−28,736.4
$Ca_2Si_2O_6$	Fe_2SiO_4	−28,573.8
$NaSi_{0.5}O_{1.5}$	Fe_2SiO_4	−4,723.9
$KAlSiO_4$	Fe_2SiO_4	22,245.0
$Ca_3(PO_4)_2$	Fe_2SiO_4	4,909.8
H_2O	Fe_2SiO_4	9,769.4
$Ca_2Si_2O_6$	Mg_2SiO_4	574.1
$NaSi_{0.5}O_{1.5}$	Mg_2SiO_4	9,272.3
$KAlSiO_4$	Mg_2SiO_4	36,512.7
$Ca_3(PO_4)_2$	Mg_2SiO_4	−6,766.8
H_2O	Mg_2SiO_4	24,630.1
$NaSi_{0.5}O_{1.5}$	$Ca_2Si_2O_6$	7,430.3
$KAlSiO_4$	$Ca_2Si_2O_6$	19,927.4
$Ca_3(PO_4)_2$	$Ca_2Si_2O_6$	88,993.1
H_2O	$Ca_2Si_2O_6$	−1,583.7
$KAlSiO_4$	$NaSi_{0.5}O_{1.5}$	−1,102.3
$Ca_3(PO_4)_2$	$NaSi_{0.5}O_{1.5}$	−13,062.6
H_2O	$NaSi_{0.5}O_{1.5}$	13,043.1
$Ca_3(PO_4)_2$	$KAlSiO_4$	85,064.0
H_2O	$KAlSiO_4$	35,572.8
H_2O	$Ca_3(PO_4)_2$	53,448.7

sets that were not included in the calibration database. We choose to examine three experimental studies to highlight the advantages and disadvantages of pMELTS in application to mantle melting.

4. Discussion

4.1. Prediction of Partial Melting Of Peridotite

[33] To illustrate the behavior of pMELTS for application to problems of partial melting of the mantle, we compare pMELTS calculations to partial melting experiments of MM3 peridotite at 1 GPa [*Baker and Stolper*, 1994; *Baker et al.*, 1995; *Hirschmann et al.*, 1998a]. An extensive comparison between MELTS calculations and these experiments is given by *Hirschmann et al.* [1998b]. The MM3 experiments were not used in the calibration of either MELTS or pMELTS. As will be seen, pMELTS calculations reproduce the experimental results more accurately than MELTS.

[34] Relative to experiments, a given melt fraction requires higher temperature in pMELTS calculations

Table 4. Corrections to Standard State Properties

Component	*H*, kJ	*S*, J/K
Si_4O_8	69.753	45.580
TiO_2	−16.941	
Al_4O_6	43.463	−25.166
Fe_2O_3	163.653	25.413
$MgCr_2O_4$	7.2386	
Fe_2SiO_4	13.739	6.424
Mg_2SiO_4	7.9119	12.777
$Ca_2Si_2O_6$	−21.863	−2.266
$NaSi_{0.5}O_{1.5}$	−20.029	
$KAlSiO_4$	−16.015	−7.311
$Ca_3(PO_4)_2$	13.197	

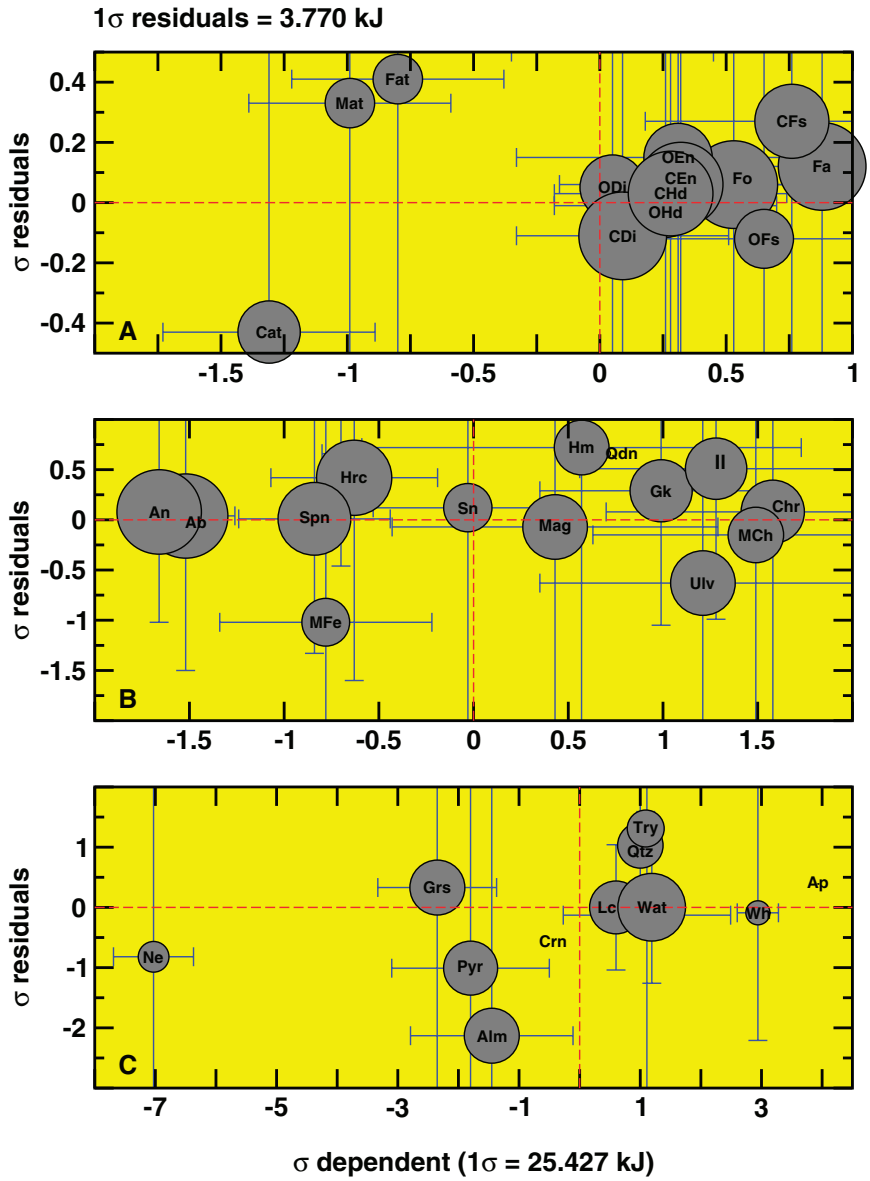

Figure 7. Analysis of residuals associated with calibration of the experimental database to the pMELTS liquid thermodynamic model. Residuals (ordinate) are expressed in units of standard deviation, where one standard deviation is 3.770 kJ and represents the uncertainty in estimation of the chemical potential of the endmember solid from the associated liquid composition at the T and P of the experiment. The abscissa is the dependent variable associated with the model inversion, which is the average contribution of liquid mixing properties to the regressed fit of solid-liquid equilibria for that mineral. It is given in units of standard deviation, where 1σ is ~25 kJ. The dashed horizontal red lines correspond to an average residual of zero. The size of the symbols reflects the number of solid-liquid pairs of that type in the calibration database. Error bars are ±2σ. Vertical displacement of a solid-liquid pair from the zero line represents systematic error.

(Figure 8). The offset ranges from negligible near 2% melting to 60°C near 10% and averages ~50°C over the range of melt fractions from 0 to 25%. This discrepancy, discussed in greater detail below, is unsatisfactory, but is reduced markedly relative to the 100°C mismatch between these experiments and MELTS calculations [*Hirschmann et al.*, 1998b].

[35] One of the chief inaccuracies of the original MELTS calibration was prediction of the concen-

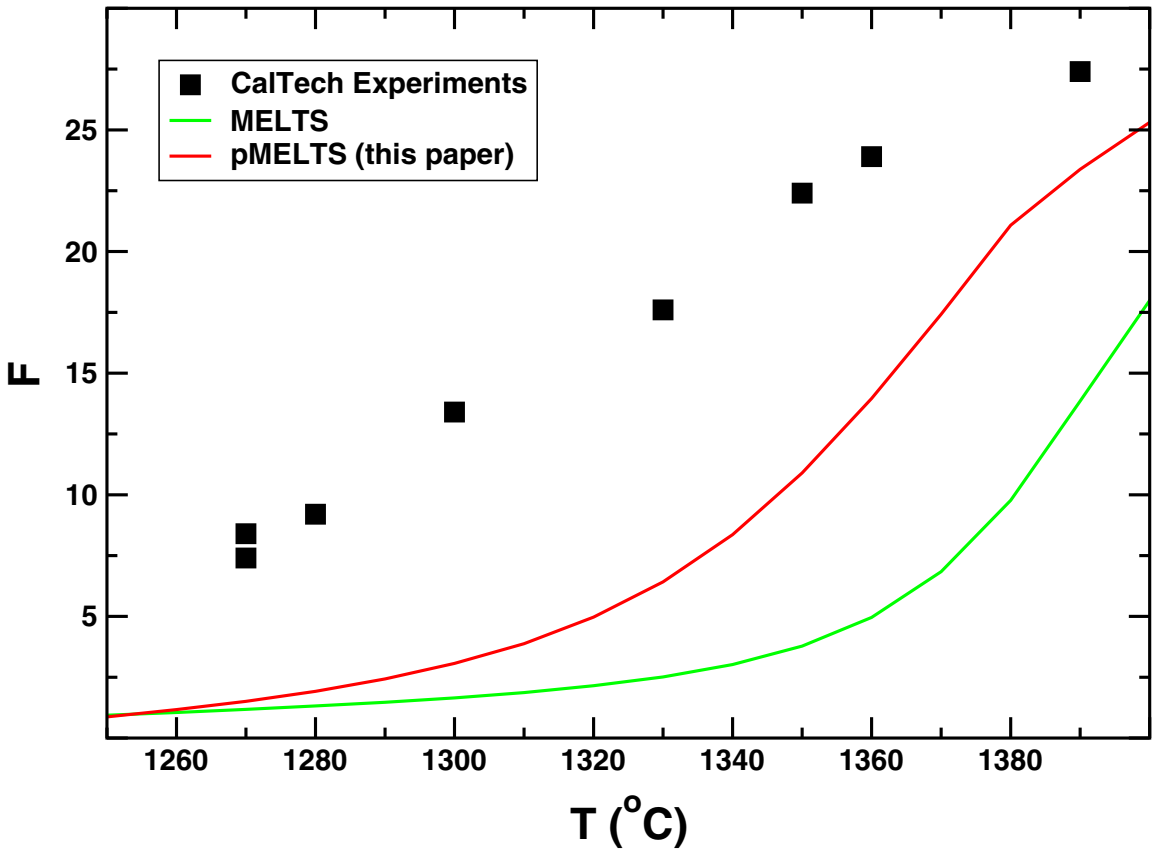

Figure 8. MELTS [*Ghiorso and Sack*, 1995] and pMELTS (this paper) estimates of the temperature dependence of the liquid fraction (*F*, in %) formed by partial melting of MM3-composition peridotite at 1 GPa compared to the experimental results reported by *Baker and Stolper* [1994] and *Hirschmann et al.* [1998a].

tration of SiO_2 in partial melts of peridotite, which was displaced to systematically lower concentrations than those indicated by experiments. Predicted SiO_2 content of partial melts coexisting with fertile lherzolite residua at 1 GPa and at modest melt fraction (5–20%) is ~51–52.5 wt%, compared with ~47% in original MELTS and 49.5–52% in the experiments (Figure 9). Over the majority of this melting range, pMELTS predictions are ~1% higher in SiO_2 than that indicated by experiments, a discrepancy that is well within the interlaboratory variability of compositions of partial melts of peridotite at modest melt fraction (see comparisons by *Kushiro* [1998]). The near-solidus increases in the silica content of the liquid indicated by experiments [*Baker et al.*, 1995; *Hirschmann et al.*, 1998a; *Kushiro*, 1996; *Pickering-Witter*, 2000; *Schwab*, 2001] and predicted by MELTS [*Baker et al.*, 1995; *Hirschmann et al.*, 1998b, 1998a] are also reproduced by the pMELTS calculations, although the magnitude of the calculated increase is less pronounced than that indicated by the experiments.

[36] Calculated liquid concentrations of other major oxides except MgO show excellent agreement with experimental liquids (Figure 10). The trends for Al_2O_3, FeO, and CaO calculated with pMELTS match the experimental trends as well as or better than trends calculated with MELTS. Predicted concentrations of Al_2O_3, CaO, and FeO all agree with experimental data to better than 1 wt%. Calculated MgO is improved relative to MELTS over much of the melting interval, except near the solidus, where the pMELTS trend predicts MgO concentrations that are too high (Figure 10). This discrepancy is partly related to the temperature offset discussed above.

[37] Minor oxides Na_2O and TiO_2 also show good agreement between calculations and experiments. The maximum in TiO_2, first noted in experiments

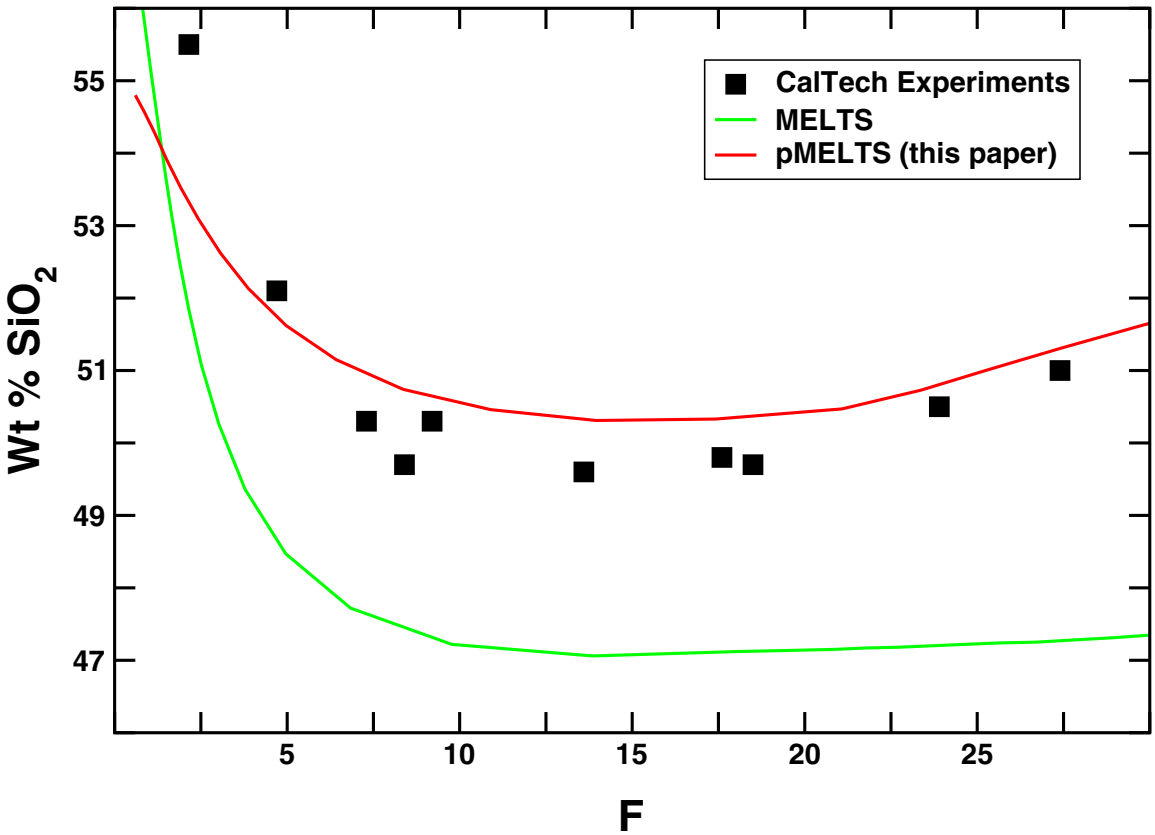

Figure 9. MELTS [*Ghiorso and Sack*, 1995] and pMELTS (this paper) estimates of the concentration of SiO_2 in liquids formed by partial melting of MM3-composition peridotite at 1 GPa compared to the experimental results reported by *Baker and Stolper* [1994] and *Hirschmann et al.* [1998a]. *F* denotes the % fraction of liquid.

and MELTS calculations in *Baker et al.* [1995] and corroborated by *Robinson et al.* [1998] and *Pickering-Witter and Johnston* [2000], is also present in pMELTS, but in pMELTS the maximum is closer to experimental observations (Figure 10a). Predicted Na_2O in the liquid also agrees well with the experiments and is much improved relative to that predicted by MELTS (Figure 9). Strong near-solidus enrichments in alkalis are expected to reduce isobaric and polybaric (adiabatic) melt productivity, relative to values prevailing at higher melt fractions [*Asimow et al.*, 1997, 2001; *Hirschmann et al.*, 1999b; *Robinson et al.*, 1998]. Because the alkali contents predicted by MELTS are exaggerated, low near-solidus productivity is also exaggerated.

[38] Calculated modes of residual minerals are compared to the MM3 experiments in Figure 11. There is excellent agreement for olivine and orthopyroxene (opx) in pMELTS. In contrast, MELTS predicts more opx and less olivine than indicated by experiments. The improved match for liquid silica concentration (Figure 9) is related to the improved match to predicted opx and olivine modes, just as the overstabilization of opx relative to olivine at 1 GPa was an important cause of the low silica liquids predicted by MELTS [*Hirschmann et al.*, 1998b]. In pMELTS, clinopyroxene (cpx) is exhausted near 21% melting, in good agreement with experiments (see CaO versus *F* plot, Figure 10) and more accurate than MELTS, which calculated cpx exhaustion to be at 18%. However, proportions of calculated cpx are too high, while that of liquid is too low. In other words, the temperature offset indicated in Figure 8 can be thought of largely as an overstabilization of cpx relative to liquid. Liquid and cpx have similar

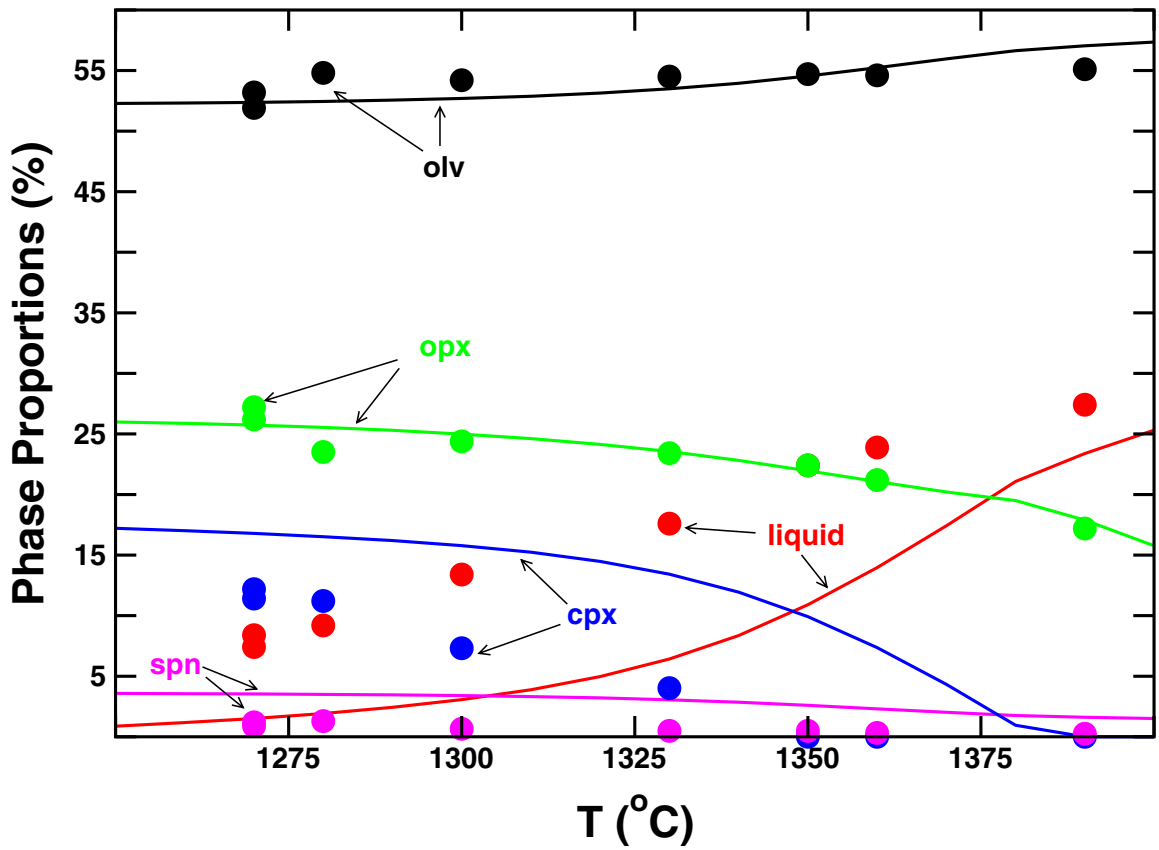

Figure 10. Compositions of partial melts estimated using pMELTS for partial melting of MM3-composition peridotite at 1 GPa compared to experimental results reported by *Baker and Stolper* [1994], *Hirschmann et al.* [1998a], and Baker (personal communication, 2000). *F* denotes the % fraction of liquid.

compositions, so discrepancies between calculated and experimental cpx and liquid modes exert small influence on predicted liquid compositions.

[39] A significant outstanding problem is that pMELTS requires higher temperatures to achieve a given melt fraction of peridotite at 1 GPa than that indicated by experiments. Notably, the maximum offset (~60°C) is reduced relative to MELTS (100°C). Although it is likely that most of the offset is the result of inaccuracies in pMELTS, a portion of the discrepancy may lie in the small but poorly characterized volatile content of most nominally anhydrous piston cylinder experiments (as discussed in section 2.1). "Phantom" volatiles may increase the amount of liquid present, thereby causing apparent underprediction of melt fraction in the corresponding anhydrous calculation. However, owing to incompatible behavior of H_2O in residual mantle minerals, H_2O concentration in the liquid, and thus its effect on melt fraction, should be greatest in the first few percent of melting. The mismatch between calculated and observed melt fractions is present to relatively high *F* (Figure 8). However, CO_2 concentrations are partially buffered by the presence of graphite and should vary less with melt fraction.

4.2. Experiments of *Falloon et al.* [1999]

[40] Experiments pertaining to partial melting of peridotite are reported by *Falloon et al.* [1999]. These experiments, performed at 1 and 1.5 GPa, were conceived as tests of the experimental results of the Caltech group on MM3 composition peridotite [e.g., *Baker and Stolper*, 1994; *Baker et al.*, 1995; *Hirschmann et al.*, 1998a]. They include both partial melting experiments and crystallization runs employing compositions similar to the partial melts described by *Baker and Stolper* [1994] and *Baker et al.* [1995]. Therefore the

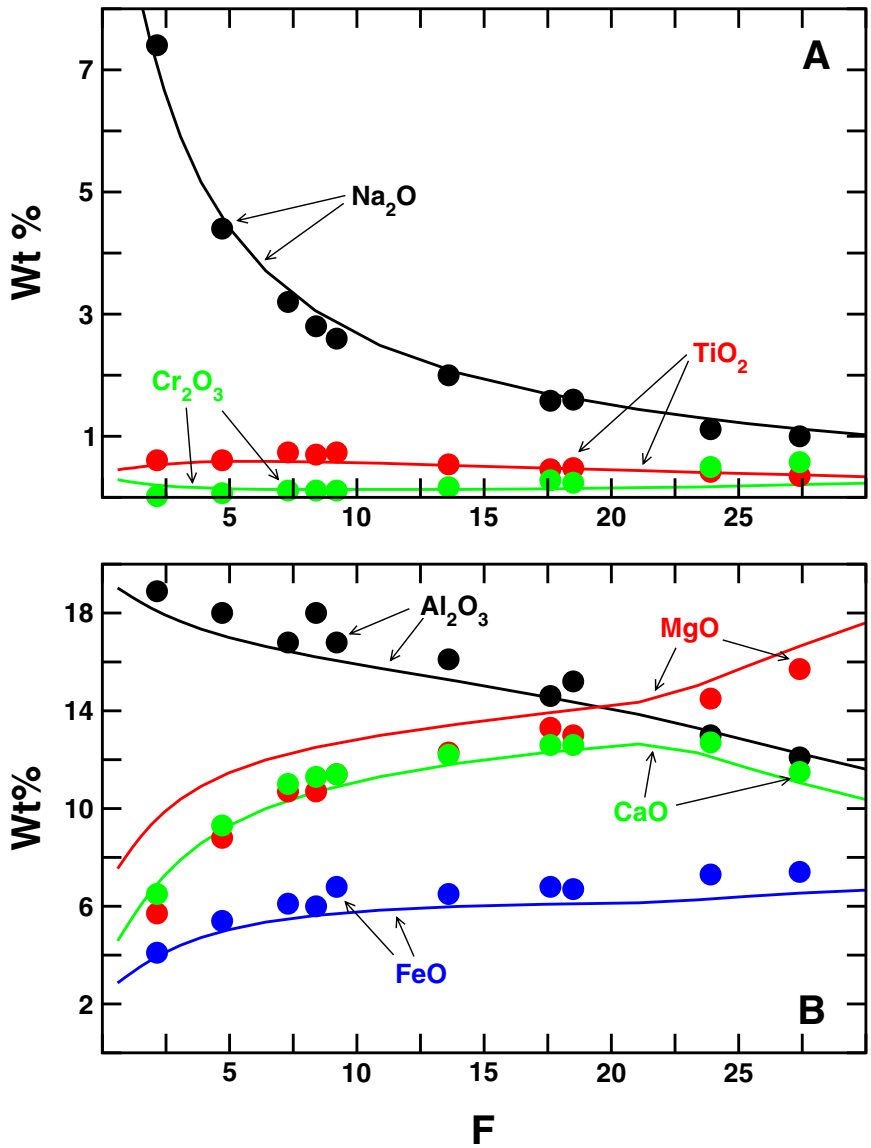

Figure 11. Phase proportions estimated using pMELTS for partial melting of MM3-composition peridotite at 1 GPa compared to experimental results reported by *Baker and Stolper* [1994] and Baker (personal communication, 2000).

Falloon et al. [1999] experiments provide the opportunity to compare the predictions of pMELTS to an independent data set with compositions and run conditions related to those of the Caltech experiments.

[41] The crystallization experiments of *Falloon et al.* [1999] were performed to test whether the glass compositions reported from 1 GPa peridotite partial melting experiments by *Baker and Stolper* [1994] and *Baker et al.* [1995] are in equilibrium with an appropriate peridotite residual assemblage at the reported conditions. *Hirschmann et al.* [1998a] presented revised analyses of glass compositions from the original experiments conducted by *Baker and Stolper* [1994] and *Baker et al.* [1995]. Because these reflect partial melt compositions more accurately than the mixtures employed by *Falloon et al.* [1999], the crystallization experiments are not a strict test of the partial melting study. However, comparison between pMELTS and these experiments may improve understanding of the relative contributions of experimental artifact and calculation bias to the mismatches described in

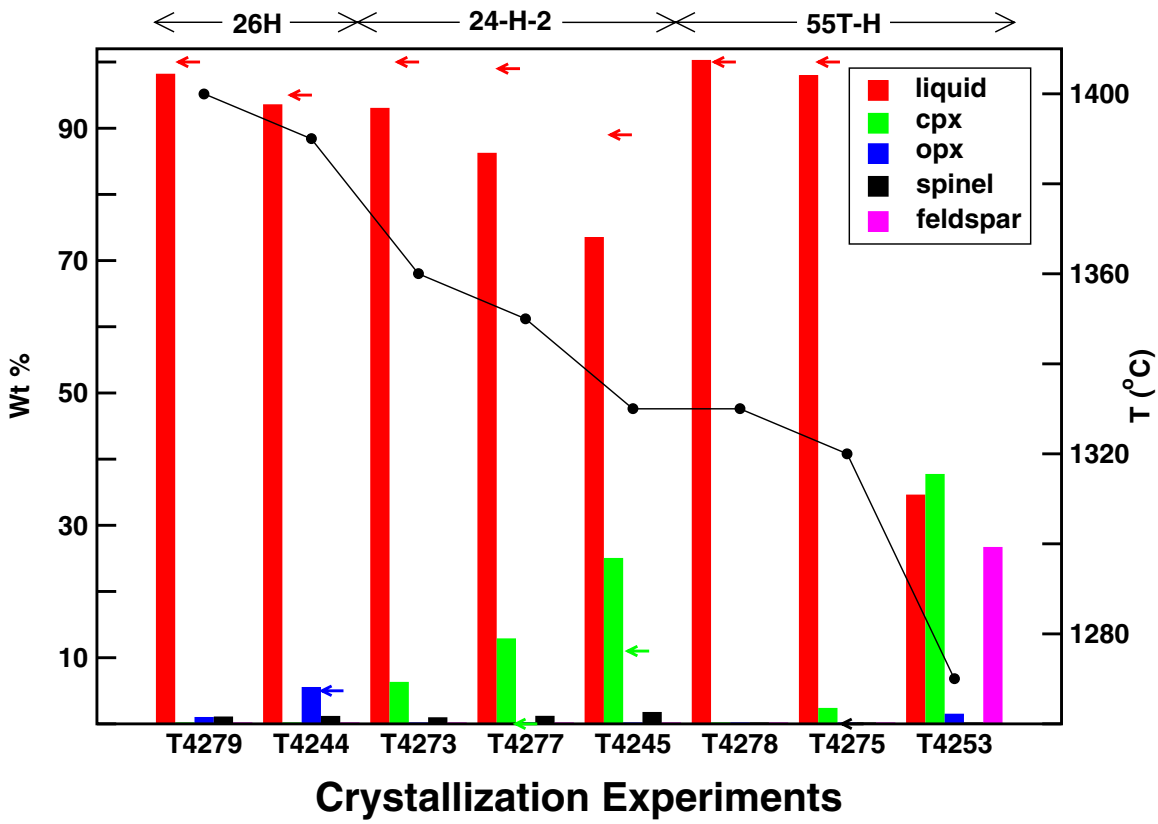

Figure 12. Comparison of pMELTS estimates of phase proportions to *Falloon et al.* [1999] results from "crystallization" experiments of MM3-derived melts at 1 GPa. Vertical bars denote pMELTS estimates and arrows indicate experimentally derived quantities. *Falloon et al.* [1999] report the assemblage liquid, cpx, opx, feldspar for experiment T4253 but give no abundance data. Numbers and labels of experiments refer to the original paper.

section 4.1. It may also provide some insight regarding the magnitude and significance of the disagreements between the two sets of experiments.

[42] We compare pMELTS calculations and *Falloon et al.*'s [1999] crystallization experiments on the same bulk composition at equivalent *T*, *P* conditions in Figure 12. Experiments T4279 and T4278 yielded ~100% liquid and corresponding pMELTS calculations predict between 94 and 100% liquid. Experiment T4244 contained ~5% opx, and this is matched by the pMELTS calculation. Experiments T4277, T4245, and T4275 all contained small amounts of cpx, and this is also predicted by pMELTS, but the predicted proportion of cpx is in all cases greater than the experimentally determined value. Experiment 4253 is reported to be highly crystalline and contain cpx, plagioclase, and olivine; pMELTS predicts ~30% glass, with cpx, plagioclase, and a small proportion of opx. Note that pMELTS predicts crystallization of small amounts of Cr-rich spinel in most cases, but spinel was not observed in the experiments. The chief discrepancies between *Falloon et al.*'s [1999] experimental results and pMELTS are that pMELTS predicts too much cpx and too little liquid. This is most evident for experiments T4273, T4277, and T4245. This discrepancy is identical to that between pMELTS and the experiments on MM3 reported by the Caltech group (summarized in section 4.1), although the comparison between pMELTS and *Falloon et al.*'s [1999] estimated proportions is more favorable. Nevertheless, these "crystallization" experiments highlight the difficulty of correctly estimating the cpx/liquid ratio in peridotite melting with pMELTS.

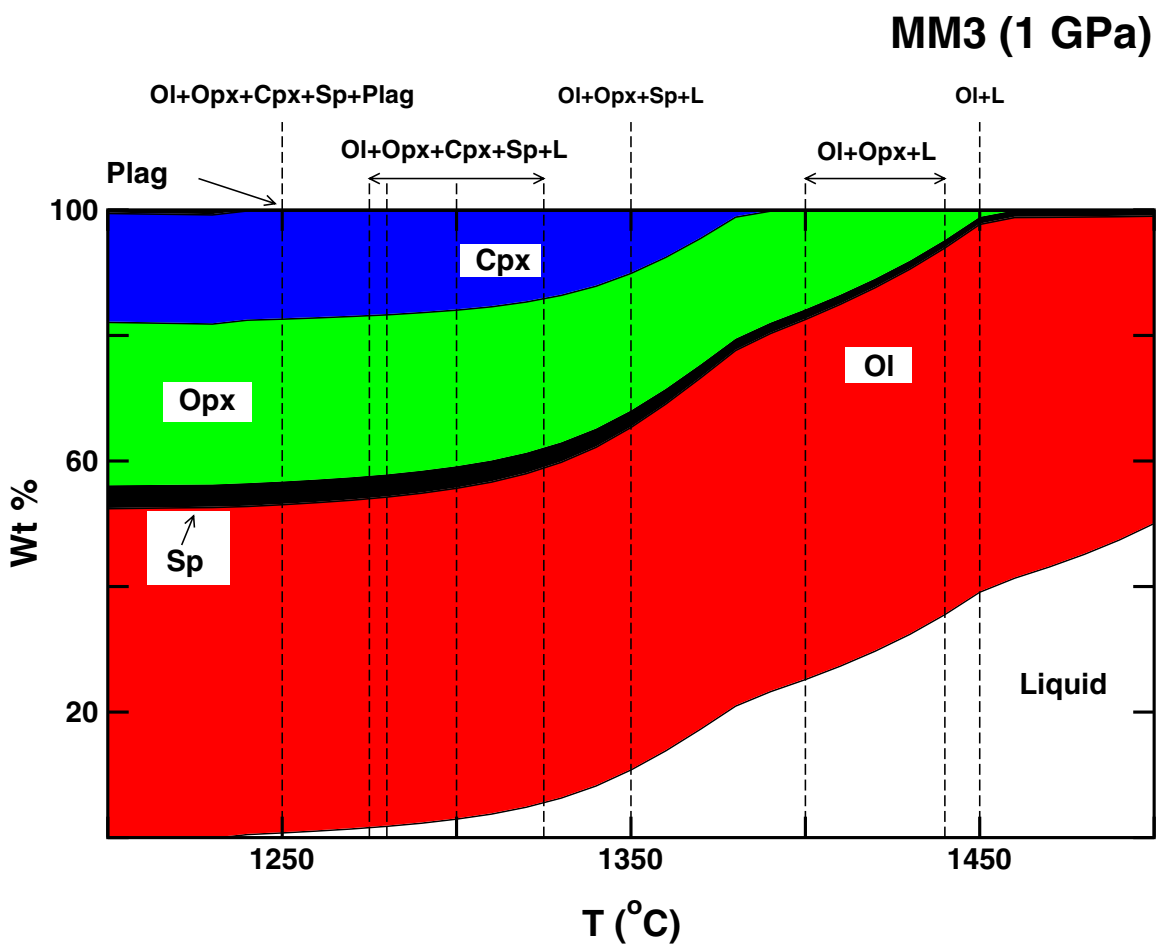

Figure 13. Estimates of phase proportions in MM3-bulk composition calculated by pMELTS compared to results of melting experiments performed by *Falloon et al.* [1999] at 1 GPa. Vertical lines are labeled by experimentally determined phase assemblages. Calculations are denoted by labeled regions.

[43] Results of the peridotite partial melting experiments of *Falloon et al.* [1999] are displayed in Figures 13, 14, and 15, along with estimates of phase proportions calculated using pMELTS. For MM3 at 1 GPa (Figure 13) the location of the onset of crystallization of olivine, opx, spinel, plagioclase and the location of the solidus compares favorably. As in the pMELTS comparison to *Falloon et al.*'s [1999] crystallization experiments, the onset of cpx crystallization appears 20°–30°C higher than experimentally indicated. Similar remarks apply to the 1.5 GPa partial melting experiments (Figure 14). The experimentally determined location of the solidus at 1.5 GPa agrees well with pMELTS calculations. Results of calculations and experiments for KLB-1 peridotite at 1 GPa are in very good agreement with the exception of onset of clinopyroxene crystallization, which is offset by about 20°C (Figure 15).

[44] In summary, pMELTS does a very good job of reproducing *Falloon et al.*'s [1999] experiments with the proviso that appearance of cpx in pMELTS is offset to higher T by ~25°C and that the cpx/liquid proportion is consequently offset during initial crystallization of cpx. As the liquid and cpx are very similar in major element composition, this discrepancy has a small effect on major element liquid composition. It is interesting to note that the partial specific Gibbs free energy calculated by pMELTS for liquid and cpx in the composition range found in these experiments is very similar, and this implies that the over-stabilization of cpx in pMELTS calculations is caused by a small energetic inaccuracy.

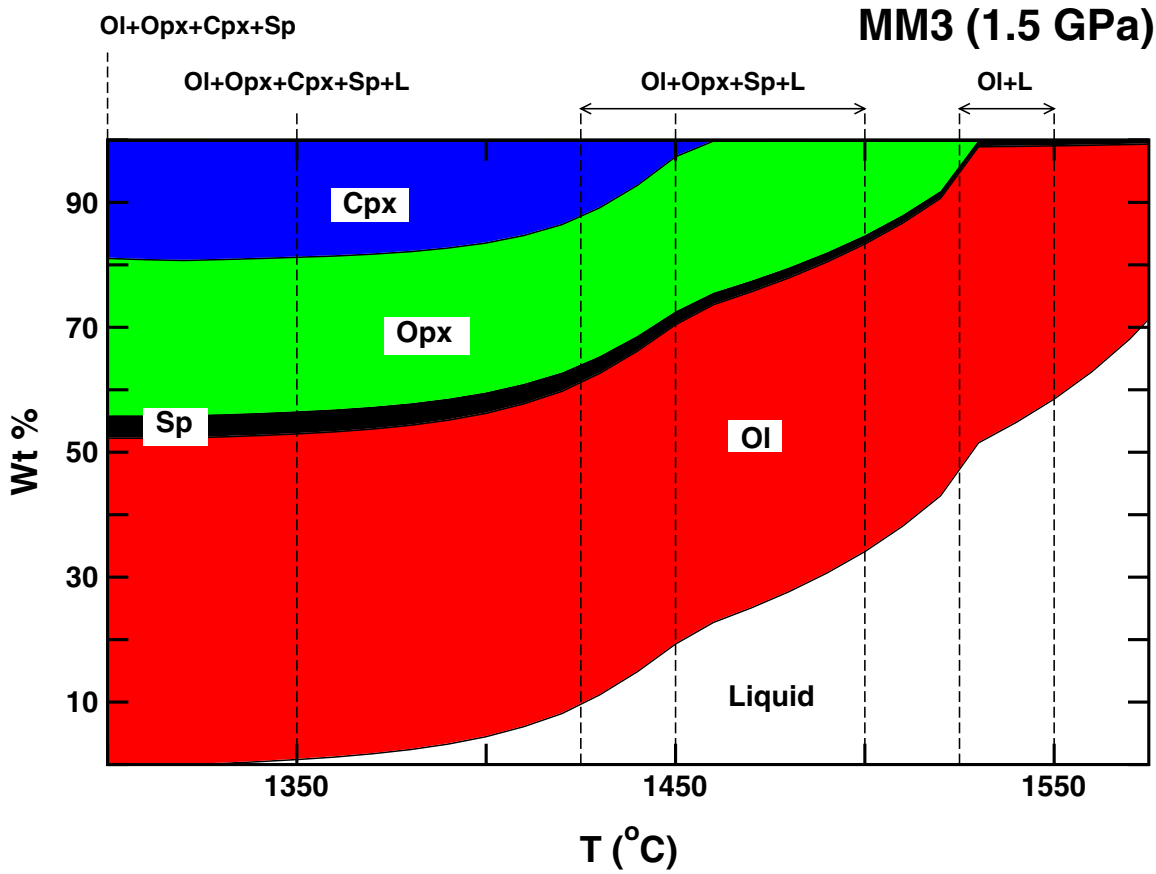

Figure 14. Estimates of phase proportions in MM3-bulk composition calculated by pMELTS compared to results of melting experiments performed by *Falloon et al.* [1999] at 1.5 GPa. Vertical lines are labeled by experimentally determined phase assemblages. Calculations are denoted by labeled regions.

[45] Comparison of pMELTS calculations to both the Caltech MM3 experiments and those of *Falloon et al.* [1999] are marred by the same inaccuracy, the overstablization of cpx in the calculations. Given the different experimental approaches of these studies and the fact that the studies include both partial melting and crystallization experiments, we infer that the problem resides with pMELTS rather than with the experimental studies. The fact that the discrepancies with the calculations are in the same sense for both studies corroborates the conclusions of *Kushiro* [2001] and of *Schwab and Johnston* [2001] that the experimental studies are largely in agreement. However, it is interesting to consider why the discrepancy between calculations and experiments is smaller for the Falloon et al. experiments than for the Caltech experiments.

[46] Compared to the Caltech experiments, those of *Falloon et al.* [1999] require systematically higher temperatures for the same phase assemblage or liquid composition. For example, whereas *Baker et al.* [1995] bracketed the 1 GPa solidus of MM3 peridotite between 1240° and 1250°C, *Falloon et al.* [1999] bracket it between 1250° and 1275°C. The crystallization experiments of *Falloon et al.* [1999] yield liquidus temperatures that are higher by as much as 50°C than those indicated by the original partial melting experiments of *Baker et al.* [1995]. Some of these differences undoubtedly reflect the near-absence of K_2O and H_2O in bulk compositions used by *Falloon et al.* [1999], as the analyses reported by *Hirschmann et al.* [1998a] indicate that these components are non-negligible in the low-melt fraction partial melting experiments from Caltech. However, as noted by *Schwab and John-*

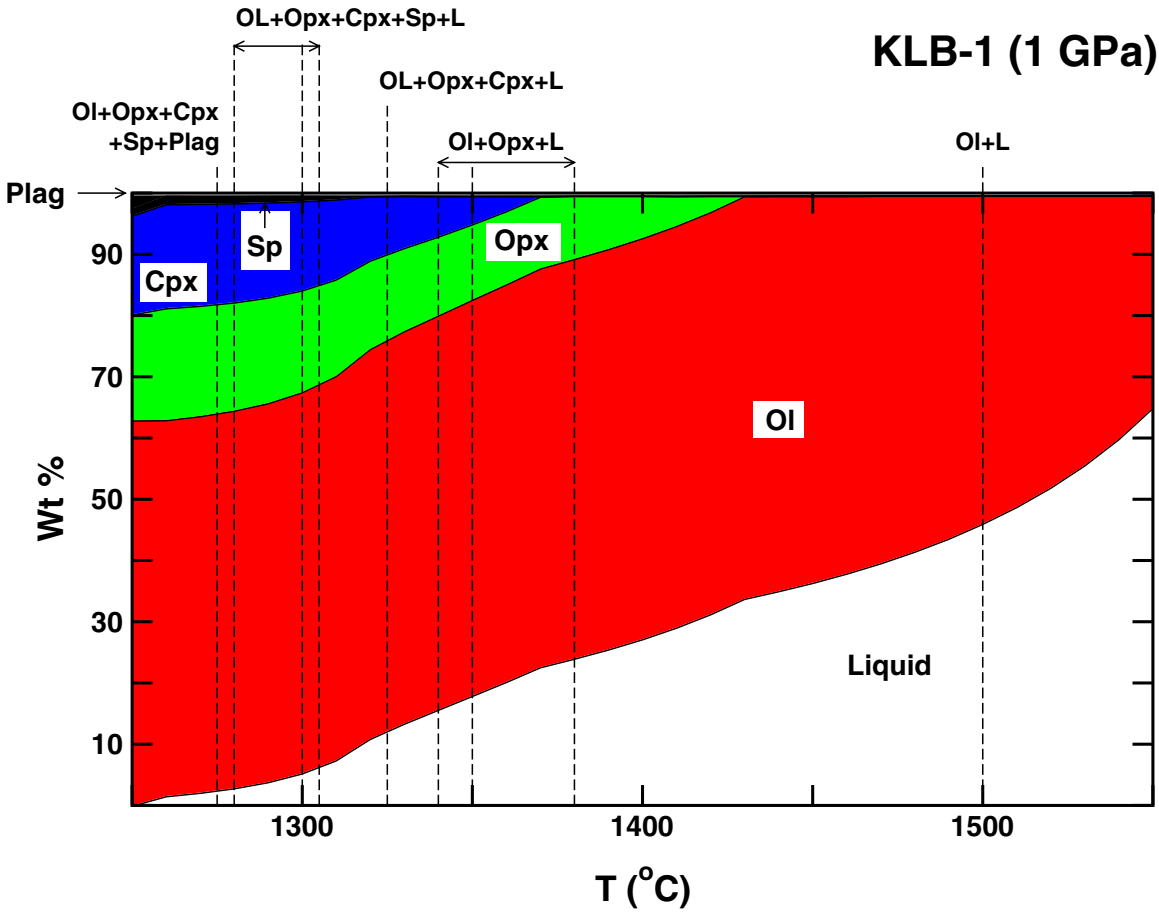

Figure 15. Estimates of phase proportions in KLB-1-bulk composition calculated by pMELTS compared to results of melting experiments performed by *Falloon et al.* [1999] at 1 GPa. Vertical lines are labeled by experimentally determined phase assemblages. Calculations are denoted by labeled regions.

ston [2001], many of the systematic differences between the Falloon et al. and Caltech experiments are almost completely eliminated when they are compared as a function of liquid MgO content rather than temperature. Because MgO concentrations in otherwise similar liquids in equilibrium with peridotite residual minerals are generally a good indicator of temperature, there may be a systematic offset in the accuracy of the W/Re thermocouples used in the two studies. Such an offset would not be surprising, given the well-known problems with accurate temperature measurement in solid-media devices discussed in section 2.1. Therefore the marginally better agreement of pMELTS with the experiments of *Falloon et al.* [1999] may suggest that a preponderance of high-pressure experiments used for calibration of pMELTS had temperature measurements more consistent with those reported by *Falloon et al.* [1999].

4.3. Garnet Peridotite Melting Experiments of *Walter* [1998]

[47] The 3–7 GPa garnet peridotite partial melting experiments of *Walter* [1998] provide an opportunity to examine extrapolation of the pMELTS calibration to higher pressures. For each mineral saturated in the experiments, we examine the calculated saturation-state of the principal components (forsterite, pyrope, etc.). In Figure 16, the departure of $\mu_i^{\text{solid}} - \mu_i^{\text{liquid}}$ from zero gives the predicted saturation affinity, with positive values representing undersaturation, negative values representing supersaturation, and zero indicating equi-

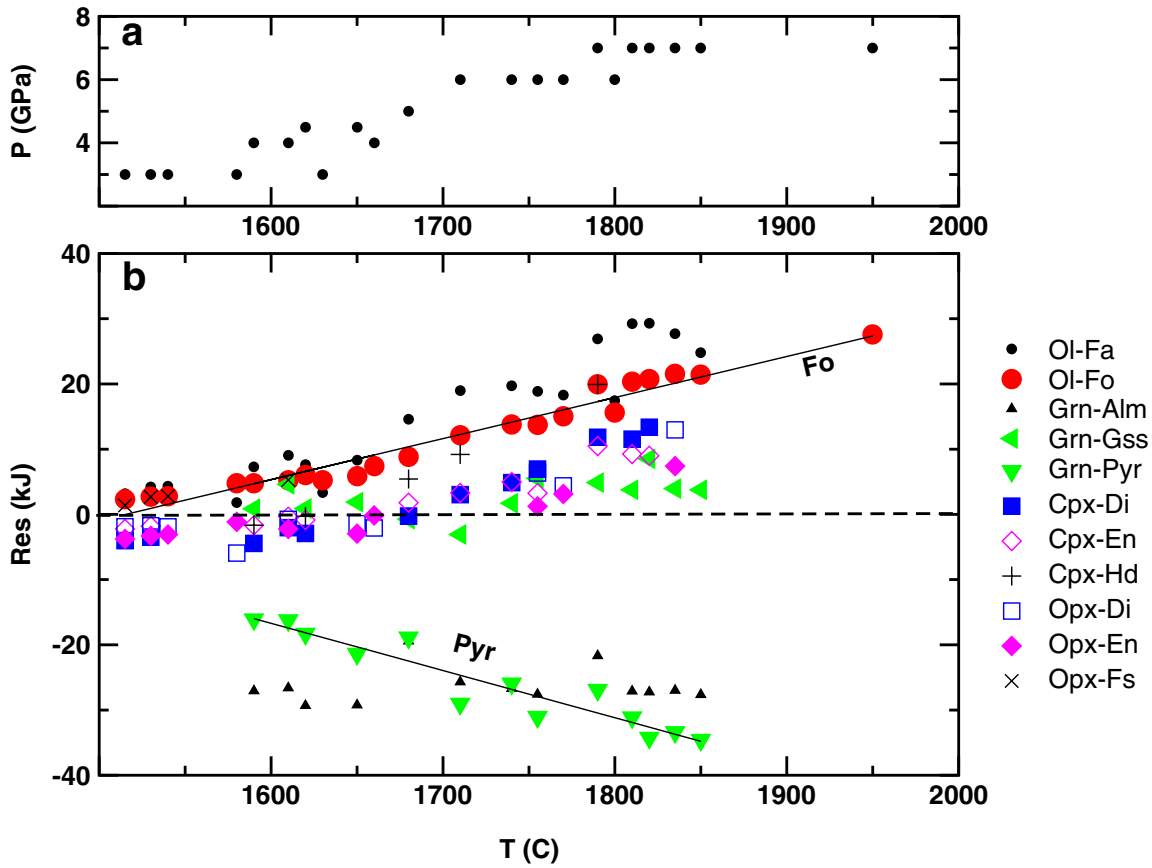

Figure 16. Analysis of experimental results from *Walter* [1998] on partial melting of peridotite to pressures of 7 GPa. Figure 16a shows pressures and temperatures of the experiments. Figure 16b shows a measure of model versus experimental misfit (ordinate, see text) plotted versus temperature of the experiment. Each data point represents a principal end-member component (e.g., Mg_2SiO_4 or Fe_2SiO_4 in olivine, $Mg_3Al_2Si3O_{12}$ in garnet, etc.) of a mineral observed in a particular experiment. The location of each data point along the ordinate, $\mu_i^{solid} - \mu_i^{liquid}$, is the difference in chemical potential of the mineral component and the weighted sum of chemical potentials of liquid components necessary to construct the mineral component stoichiometry. Thus, according to the calculation, mineral end-members that plot above the zero-line are undersaturated, and those that plot below are super-saturated. To illustrate the relationship between relative degrees of supersaturation or undersaturation, we can examine one of the most pronounced discrepancies between the calculations and Walter's experiments: at 1835°C and 7 GPa, run 70.09 produced liquid, olivine, garnet and orthopyroxene (the vertical cluster of points third from the left). If pMELTS is run with the reported liquid composition at the experimental *T* and *P*, the result is ~23 wt % garnet and 77 wt % residual liquid. In order to bring olivine into saturation with the reported liquid composition in pMELTS, the temperature must be lowered to 1514°C. Similarly orthopyroxene and clinopyroxene saturation are calculated when *T* is lowered to 1775°C and 1722°C, respectively. The temperature has to be raised to 2177°C to bring garnet into calculated equilibrium with this liquid.

librium (see Figure 16 caption for further details). For pyroxene components, calculated departures from equilibrium are small to pressures of 6 GPa ($T \sim 1775$°C), indicating that pyroxene-liquid equilibria are well modeled by pMELTS up to this pressure. However, olivine and garnet saturation are not reproduced accurately and the mismatch increases with pressure. Olivine becomes increasingly undersaturated with increasing pressure. The greater scatter in residuals for fayalite relative to those for forsterite are a consequence of the low fayalite concentration in calculated olivine compositions and of uncertainties regarding the oxygen fugacities of the experiments. With pressure, the pyrope and almandine (but not grossular) components of garnet become increasingly supersaturated. These systematic discrepancies demonstrate that the deficiencies of pMELTS become more pro-

nounced with increasing pressure in the garnet peridotite facies.

[48] The underlying cause of the failure in pMELTS over the 3–7 GPa pressure interval is difficult to isolate with certainty, but there is considerable reason to suspect that it lies in the assumed equation of state for the liquid. The problem is not likely to be from the assumed energetic response of the minerals to increasing pressure, as the EOSs for forsterite and pyrope are known to pressures of 10 GPa [*Berman*, 1988]; although calibration points are restricted to $T < 1000°C$. It is plausible that the cause is in the model for the entropy of the liquid and that the apparent failure at high pressure is in fact a failure at high temperature (e.g., Figure 16a). For example, the systematic misfits for olivine and garnet components illustrated in Figure 16b can be accounted for by a correction to the partial molar entropy of the X_2SiO_4 and $X_3Al_2Si_3O_{12}$ liquid "components" of 62 and −60 J/K, respectively. These represent extraordinarily large corrections; in the case of olivine, they are comparable in magnitude to the entropy of fusion. If the values for the entropy of these liquid components were so far from correct, we would expect a pronounced temperature-dependence to the residuals for the subset of the mineral-liquid calibration data from low pressure and this is not the case for either component of the olivine. It thus seems likely that the misfit arises from the choice of the liquid EOS. Correcting the offsets in Figure 16b requires adjustment to the partial molar volume of X_2SiO_4 and $X_3Al_2Si_3O_{12}$ components of -7×10^{-6} and $+4 \times 10^{-6}$ m^3/mol, respectively. Although these corrections are not small, they are plausible under the assumption that the pressure derivative of the compressibility of silicate melts is a strong function of pressure and composition.

[49] Recall from the discussion above that the liquid EOS chosen for pMELTS is defined by volumetric and derivative property measurements at 10^5 Pa, a model equation corresponding to a 3rd-order Birch-Murnaghan EOS (equation (4)), and an estimate of K'; derived from high-pressure density determinations on molten liquids. Critical to application of the Birch-Murnaghan EOS to the liquid state is an understanding that the compressibility of the melt is much larger than the compressibility of the corresponding solid, and this results in compressions on the order of 30% at 10 GPa. Consequently, in the case of a liquid, the K'; in (4) becomes an influential parameter at pressures as low as 3 Gpa, and it is the only parameter in the Birch-Murnaghan EOS that compensates for the volumetric consequences of coordination changes of cations in the melt with pressure. Our assumption that K'; is independent of both pressure and composition is undoubtedly a gross simplification which may very well be the cause of the failure pMELTS at pressures greater than 3 GPa.

[50] In our view it is likely that the residual patterns displayed by *Walter*'s [1998] data set in Figure 16b point to the need for a more sophisticated description of the EOS of silicate liquids at pressures in excess of 3 GPa. The K' value in these liquids must certainly be compositionally dependent as has been found by researchers who have attempted to apply the Birch-Murnaghan EOS to fusion curve analysis in simpler systems [e.g., *Rigden et al.*, 1989] and is also likely to be temperature dependent. In addition, structural changes in the liquid induced by pressure will probably require a pressure dependence of K'; or abandonment of the Birch-Murnaghan form entirely and adoption of an alternative EOS. One promising refinement is the adoption of a homogenous speciation model for the liquid phase that explicitly accounts for pressure-induced coordination shifts of cations. These considerations are the subject of ongoing research in extending MELTS/pMELTS to higher-pressure conditions. The conclusion to be drawn at this stage from analysis of *Walter*'s [1998] multianvil data is not to apply pMELTS at pressures in excess of 3 GPa without due consideration of the phases involved and the likely errors that will arise.

Appendix A. Data Sources for the pMELTS Calibration Database

[51] Asterisks indicate Post-MELTS data sources.

[52] Agee, C. B., and D. Walker, Aluminum partitioning between olivine and ultrabasic silicate liquid to 6 GPa, *Contrib. Mineral. Petrol.*, *105*, 243–254, 1990.

[53] Arndt, N. T., Partitioning of nickel between olivine and ultrabasic and basic komatiite liquids, *Carnegie Inst. Washington Year Book.*, *76*, 553–557, 1977.

[54] *Auwera, J. V., and J. Longhi, Experimental study of a jotunite (hypersthene monzodiorite): Constraints on the parent magma composition and crystallization conditions (P,T, fO2) of the Bjerkreim-Sokndal layered intrusion (Norway), *Contrib. Mineral. Petrol.*, *118*, 60–78, 1994.

[55] Baker, D. R., and D. H. Eggler, Compositions of anhydrous and hydrous melts coexisting with plagioclase, augite, and olivine or low-Ca pyroxene from 1 atm to 8 kbar: Applications to the Aleutian volcanic center of Atka, *Am. Mineral.*, *72*, 12–28, 1987.

[56] *Baker, L. L., and M. J. Rutherford, The effect of dissolved water on the oxidation state of silicic melts, *Geochim. Cosmochim. Acta*, *60*, 2179–2187, 1996.

[57] *Baker, M. B., T. L. Grove, and R. Price, Primitive basalts and andesites from the Mt. Shasta region, N. California: Products of varying melt fraction and water content, *Contrib. Mineral. Petrol.*, *118*, 111–129, 1994.

[58] Barnes, S. J., The distribution of chromium among orthopyroxene, spinel and silicate liquid at atmospheric pressure, *Geochim. Cosmochim. Acta*, *50*, 1889–1909, 1986.

[59] Bartels, K. S., and T. L. Grove, High-pressure experiments on magnesian eucrite compositions: Constraints on magmatic processes in the eucrite parent body, *Proc. Lunar Planet. Sci. Conf.*, *21st,* 351–365, 1991.

[60] Bartels, K., R. J. Kinzler, and T. L. Grove, High-pressure phase relations of primitive high-aluminum basalts from Medicine Lake Volcano, Northern California, *Contrib. Mineral. Petrol.*, *108*, 253–270, 1991.

[61] Bender, J. F., F. N. Hodges, and A. E. Bence, Petrogenesis of basalts from the FAMOUS area: Experimental study from 0 to 15 kbars, *Earth Planet. Sci. Lett.*, *41*, 277–302, 1978.

[62] Bickle, M. J., Melting experiments on peridotitic komatiites, *Prog. Exper. Petrol. NERC Pub. Ser. D*, *11*, 187–195, 1978.

[63] Biggar, G. M., M. J. O'Hara, A. Peckitt, and D. J. Humphries, Lunar lavas and the achondrites: Petrogenesis of protohypersthene basalts in the maria lava lakes, *Proc. Lunar Planet. Sci. Conf.*, *2nd,* 617–643, 1971.

[64] Burnham, C. W., and R. H. Jahns, A method for determining the solubility of water in silicate liquids, *Am. J. Sci.*, *260*, 721–745, 1962.

[65] Chen, H.-K., J. W. Delano, and D. H. Lindsley, Chemistry and phase relations of VLT volcanic glasses from Apollo 14 and Apollo 17, *Proc. Lunar Planet. Sci. Conf. 13th, Part 1, J. Geophys. Res.*, *87 suppl.*, A171–A181, 1982.

[66] Delano, J. W., Experimental melting relations of 63545, 76015, and 76055, *Proc. Lunar Planet. Sci. Conf.*, *8th,* 2097–2123, 1977.

[67] Draper, D. S., and A. D. Johnston, Anhydrous PT phase relations of an Aleutian high-MgO basalt: An investigation of the role of olivine-liquid reaction in the generation of arc high-alumina basalts, *Contrib. Mineral. Petrol.*, *112*, 501–519, 1992.

[68] *Dunn, T., and C. Sen, Mineral/matrix partition coefficients for orthopyroxene, plagioclase, and olivine in basaltic to andesitic systems: A combined analytical and experimental study, *Geochim. Cosmochim. Acta*, *58*, 717–733, 1994.

[69] Fram, M. S., and J. Longhi, Phase equilibria of dikes associated with Proterozoic anorthosite complexes, *Am. Mineral.*, *77*, 605–616, 1992.

[70] Fujii, T., and H. Bougalt, Melting relations of an abyssal tholeiite and the origin of MORBs, *Earth Planet. Sci. Lett.*, *62*, 283–295, 1983.

[71] Fujii, T., and C. M. Scarfe, Composition of liquids coexisting with spinel lherzolite at 10 kbar and the genesis of MORBs, *Contrib. Mineral. Petrol.*, *90*, 18–28, 1985.

[72] *Gaetani, G. A., and T. L. Grove, The influence of water on melting of mantle peridotite, *Contrib. Mineral. Petrol.*, *131*, 323–346, 1998.

[73] *Gardner, J. E., M. Rutherford, and S. Carey, Experimental constraints on pre-eruptive water contents and changing magma storage prior to explosive eruptions of Mount St Helens volcano, *Bull. Volcanol.*, *57*, 1–17, 1995.

[74] Gee, L. L., and R. O. Sack, Experimental petrology of melilite nephelinites, *J. Petrol.*, *29*, 1233–1255, 1988.

[75] *Gerke, T. L., and A. I. Kilinc, Enrichment of SiO_2 in rhyolites by fractional crystallization: An experimental study of peraluminous granitic rocks from the St. Francois Mountains, Missouri, USA, *Lithos*, *29*, 273–283, 1993.

[76] Grove, T. L., and D. W. Beaty, Classification, experimental petrology and possible volcanic histories of the Apollo 11 high-K basalts, *Proc. Lunar Planet. Sci. Conf.*, *11th,* 149–177, 1980.

[77] Grove, T. L., and A. E. Bence, Experimental study of pyroxene-liquid interaction in quartz normative basalt 15597, *Proc. Lunar Planet. Sci. Conf.*, *8th,* 1549–1579, 1977.

[78] Grove, T. L., and W. B. Bryan, Fractionation of pyroxene-phyric MORB at low pressure: An experimental study, *Contrib. Mineral. Petrol.*, *84*, 293–309, 1983.

[79] Grove, T.L., and T.C. Juster, Experimental investigations of low-Ca pyroxene stability and olivine-pyroxene-liquid equilibria at 1-atm in natural basaltic and andesitic liquids, *Contrib. Mineral. Petrol.*, *103*, 287–305, 1989.

[80] Grove, T. L., and M. Raudsepp, Effects of kinetics on the crystallization of quartz normative basalt 15597: An experimental study, *Proc. Lunar Planet. Sci. Conf.*, *9th,* 585–599, 1978.

[81] Grove, T. L., D. C. Gerlach, and T. W. Sando, Origin of calc-alkaline series lavas at Medicine Lake Volcano by fractionation, assimilation, and mixing, *Contrib. Mineral. Petrol.*, *84*, 160–182, 1982.

[82] Grove, T. L., R. J. Kinzler, and W. B. Bryan, Fractionation of mid-ocean ridge basalt (MORB), in *Mantle Flow and Melt Generation at Mid-ocean Ridges*, *Geophys. Monogr. Ser.*,vol. 71, edited by J. Pyhipps Morgan et al., pp. 281–310, AGU, Washington, D.C., 1992.

[83] *Grove, T. L., J. M. Donnelly-Nolan, and T. Housh, Magmatic processes that generated the rhyolite of Glass Mountain, Medicine Lake volcano, N. Californica, *Contrib. Mineral. Petrol.*, *127*, 205–223, 1997.

[84] Hamilton, D. L., C. W. Burnham, and E. F. Osborn, The solubility of water and effects of oxygen fugacity and water content on crystallization in mafic magmas, *J. Petrol.*, *5*, 21–39, 1964.

[85] Helz, R. T., Phase relations of basalts in their melting range at PH_2O = 5 kb as a function of oxygen fugacity, Part II, Melt compositions, *J. Petrol.*, *17*, 139–193, 1976.

[86] Hess, P. C., M. J. Rutherford, and H. W. Campbell, Ilmenite crystallization in nonmare basalt: Genesis of KREEP and high-Ti mare basalt, *Proc. Lunar Planet. Sci. Conf.*, *9th,* 705–724, 1978.

[87] *Hirose, K., and I. Kushiro, Partial melting of dry peridotites at high pressures: Determination of compositions of melts segregated from peridotite using aggregates of diamond, *Earth Planet. Sci. Lett.*, *114*, 477–489, 1993.

[88] *Holtz, F., G. Behrens, D. B. Dingwell, and R. P. Taylor, Water solubility in aluminosilicate melts of haplogranite composition at 2 kbar, *Chem. Geol.*, *96*, 289–302, 1992.

[89] Housh, T. B., and J. F. Luhr, Plagioclase-melt equilibria in hydrous systems, *Am. Mineral.*, *76*, 477–492, 1991.

[90] Johnston, A. D., Anhydrous P-T phase relations of near-primary high-alumina basalt from the South Sandwich Islands: Implications for the origin of island arcs and tonalite-trondhjemite ser-

ies rocks, *Contrib. Mineral. Petrol*., *92*, 368–382, 1986.

[91] Jurewicz, A. J. G., D. W. Mittlefehldt, and J. H. Jones, Experimental partial melting of the Allende (CV) and Murchison (CM) chondrites and the origin of asteroidal basalts, *Geochim. Cosmochim. Acta*, *57*, 2123–2139, 1993.

[92] *Jurewicz, A. J. G., D. W. Mittlefehldt, and J. H. Jones, Experimental partial melting of the St. Severin (LL) and Lost City (H) chondrites, *Geochim. Cosmochim. Acta*, *59*, 391–408, 1995.

[93] Juster, T. C., T. L. Grove, and M. R. Perfit, Experimental constraints on the generation of FeTi basalts, andesites, and rhyodacites at the Galapagos Spreading Center, 85°W and 95°W, *J. Geophys. Res*., *87*, 9521–9574, 1989.

[94] Kelemen, P. B., D. B. Joyce, J. D. Webster, and J. R. Holloway, Reaction between ultramafic rock and fractionating basaltic magma, II, Experimental investigation of reaction between olivine tholeiite and harzburgite at 1150–1050°C and 5 kb, *J. Petrol*., *31*, 99–134, 1990.

[95] Kennedy, A. K., T. L. Grove, and R. W. Johnson, Experimental and major element constraints on the evolution of lavas from Lihir Island, Papua New Guinea, *Contrib. Mineral. Petrol*., *104*, 772–734, 1990.

[96] Kesson, S. E., Mare basalts: Melting experiments and petrogenetic interpretations, *Proc. Lunar Planet. Sci. Conf*., *16th,* 921–944, 1975.

[97] Khitarov, N. I., E. B. Lebedev, E. V. Regarten, and R. V. Arseneva, Solubility of water in basaltic and granitic melts, *Geochemistry*, *5*, 479–492, 1959.

[98] *Kinzler, R. J., Melting of mantle peridotite at pressures approaching the spinel to garnet transition: Application to mid-ocean ridge basalt petrogenesis, *J. Geophys. Res*., *102*, 853–874, 1997.

[99] Kinzler, R. J., and T. L. Grove, Crystallization and differentiation of Archean komatiite lavas from northeast Ontario: Phase equilibrium and kinetic studies, *Am. Mineral*., *70*, 40–51, 1985.

[100] Kinzler, R. J., and T. L. Grove, Primary magmas of mid-ocean ridge basalts, 1, Experiments and methods, *J. Geophys. Res*., *97*, 6885–6906, 1992.

[101] *Kushiro, I., Partial melting of a fertile mantle peridotite at high pressures: An experimental study using aggregates of diamond, in *Earth Processes: Reading the Isotopic Code*, *Geophys. Monogr. Ser.,* vol. 95, edited by A. Basu and S. Hart, pp. 109–122, AGU, Washington, D.C., 1996.

[102] Leeman, W. P., Part I Petrology of basaltic lavas from the Snake River plain, Idaho and Part II Experimental determination of partitioning of divalent cations between olivine and basaltic liquid, Ph.D. Dissertation thesis, University of Oregon, Eugene, 1974.

[103] *Longhi, J., Liquidus equilibria of some primary lunar and terrestrial melts in the garnet stability field, *Geochim. Cosmochim. Acta*, *59*, 2375–2386, 1995.

[104] Longhi, J., and V. Pan, A reconnaisance study of phase boundaries in low-alkali basaltic liquids, *J. Petrol*., *29*, 115–147, 1988.

[105] Longhi, J., and V. Pan, The parent magmas of the SNC meteorites, *Proc. Lunar Planet. Sci. Conf*., *19th,* 451–464, 1989.

[106] Longhi, J., D. Walker, T. L. Grove, E. M. Stolper, and J. F. Hays, The petrology of the Apollo 17 mare basalts, *Proc. Lunar Planet. Sci. Conf*., *5th,* 1447–1469, 1974.

[107] Longhi, J., D. Walker, and J. F. Hays, The distribution of Fe and Mg between olivine and lunar basaltic liquids, *Geochim. Cosmochim. Acta*, *42*, 1545–1558, 1978.

[108] Longhi, J., J. L. Wooden, and V. Pan, The petrology of high-Mg dikes from the Beartooth Mountains, Montana: A search for the parental magma of the Stillwater Complex, *Proc. Lunar Planet. Sci. Conf., 14th, J. Geophys. Res*., *88,* suppl., 1983.

[109] Luhr, J. F., Experimental phase relations of water- and sulfur-saturated arc magmas and the 1982 eruptions of El Chichón volcano, *J. Petrol*., *31*, 1071–1114, 1990.

[110] Mahood, G. A., and D. R. Baker, Experimental constraints on depths of fractionation of midly alkalic basalts and associated felsic rocks: Pantelleria, Strait of Sicily, *Contrib. Mineral. Petrol.*, *93*, 251–264, 1986.

[111] Meen, J. K., Formation of shoshonites from calcalkaline basalt magmas: Geochemical and experimental constraints from the type locality, *Contrib. Mineral. Petrol.*, *97*, 333–351, 1987.

[112] Meen, J. K., Elevation of potassium content of basaltic magma by fractional crystallization: The effect of pressure, *Contrib. Mineral. Petrol.*, *104*, 309–331, 1990.

[113] *Moore, G., R..K., and I.S.E. Carmichael, The effect of dissolved water on the oxidation state of iron in natural silicate liquids, *Contrib. Mineral. Petrol.*, *120*, 170–179, 1995.

[114] Murck, B. W., and I. H. Campbell, The effects of temperature, oxygen fugacity and melt composition on the behavior of chromium in basic and ultrabasic melts, *Geochim. Cosmochim. Acta*, *50*, 1871–1888, 1986.

[115] Naney, M. T., Phase equilibria of rock–forming ferromagnesian silicates in granitic systems, *Am. J. Sci. 283*, 993–1033, 1983.

[116] *Panjasawatwong, Y., L. V. Danyushevsky, A. J. Crawford, and K. L. Harris, An experimental study of the effects of melt composition on plagioclase-melt equilibria at 5 and 10 kbar: Implications for the origin of magmatic high-An plagioclase, *Contrib. Mineral. Petrol.*, *118,* 420–432, 1995.

[117] *Patino-Douce, A. E., and J. S. Beard, Dehydration-melting of biotite gneiss and quartz amphibolite from 3 to 15 kbar, *J. Petrol.*, *36*, 707–738, 1995.

[118] *Putirka, K., M. Johnson, R. Kinzler, J. Longhi, and D. Walker, Thermobarometry of mafic igneous rocks based on clinopyroxene-liquid equilibria, 0–30 kbar, *Contrib. Mineral. Petrol.*, *123*, 92–108, 1996.

[119] *Rapp, R. P., and E. B. Watson, Dehydration melting of metabasalt at 8–32 kbar: Implications for continental growth and crust-mantle recycling, *J. Petrol.*, *36*, 891–931, 1995.

[120] Rhodes, J. M., G. E. Lofgren, and D. P. Smith, One atmosphere melting experiments on ilmenite basalt 12008, *Proc. Lunar Planet. Sci. Conf.*, *5th,* 407–422, 1979.

[121] *Robinson, J. A. C., B. J. Wood, and J. D. Blundy, The beginning of melting of fertile and depleted peridotite at 1.5 GPa, *Earth Planet. Sci. Lett.*, *155*, 97–111, 1998.

[122] Roeder, P. L., Activity of iron and olivine solubility in basaltic liquids, *Earth Planet. Sci. Lett.*, *23*, 397–410, 1974.

[123] Roeder, P. L., and I. Reynolds, Crystallization of chromite and chromium solubility in basaltic melts, *J. Petrol.*, *32*, 909–934, 1991.

[124] Sack, R. O., D. Walker, and I. S. E. Carmichael, Experimental petrology of alkalic lavas: Constraints on cotectics of multiple saturation in natural basic liquids, *Contrib. Mineral. Petrol.*, *96*, 1–23, 1987.

[125] Seifert, S., H. S. C. O'Neill, and G. Brey, The partitioning of Fe, Ni and Co between olivine, metal, and basaltic liquid: An experimental and therrmodynamic investigation, with application to the composition of the lunar core, *Geochim. Cosmochim. Acta*, *52*, 603–615, 1988.

[126] *Sen, C., and T. Dunn, Dehydration melting of a basaltic composition amphibolite at, 1.5 and, 2.0 GPa: implications for the origin of adakites, *Contrib. Mineral. Petrol.*, *117*, 394–409, 1994.

[127] Sisson, T. W., and T. L. Grove, Experimental investigations of the role of H_2O in calc-alkaline differentiation and subduction zone magmatism, *Contrib. Mineral. Petrol.*, *113*, 143–166, 1993.

[128] *Snyder, D., and I. S. E. Carmichael, R. A. Weibe, Experimental study of liquid evolution in an Fe-rich, layered mafic intrusion: Constraints of Fe-Ti oxide precipitation on the T-fO2 and T-rho paths of tholeiitic magmas, *Contrib. Mineral. Petrol.*, *113*, 73–86, 1993.

[129] Stolper, E. M., Experimental petrology of eucrite meteorites, *Geochim. Cosmochim. Acta*, *41*, 587–611, 1977.

[130] Stolper, E. M., A phase diagram for mid-ocean ridge basalts: Preliminary results and impli-

cations for petrogenesis, *Contrib. Mineral. Petrol.*, *74*, 13–27, 1980.

[131] Takahashi, E., Melting relations of an alkali-olivine basalt to 30 kbars, and their bearing on the origin of alkali basalt magmas, *Carnegie Inst. Washington Year Book*, *79*, 271–276, 1980.

[132] Takahashi, E., Melting of dry peridotite KLB-1 up to 14 GPa: Implications on the origin of peridotitic upper mantle, *J. Geophys. Res.*, *91*, 9367–9382, 1986.

[133] Takahashi, E., and I. Kushiro, Melting of dry peridotite at high pressures and basalt magma genesis, *Am. Mineral.*, *68*, 859–879, 1983.

[134] Thompson, R. N., Primary basalts and magma genesis, *Contrib. Mineral. Petrol.*, *45*, 317–345, 1974.

[135] *Thy, P., High and low pressure phase equilibria of a mildly alkalic lava from the 1965 Surtsey eruption: Experimental results, *Lithos*, *26*, 223–243, 1991.

[136] *Thy, P., Experimental constraints on the evolution of transitional and mildly alkalic basalts: Crystallization of spinel, *Lithos*, *36*, 103–114, 1995a.

[137] *Thy, P., Low-pressure experimental constraints on the evolution of komatiites, *J. Petrol.*, *36* 1529–1548, 1995b.

[138] *Thy, P., and G. E. Lofgren, Experimental constraints on the low-pressure evolution of transitional and mildly alkalic basalts: Multisaturated liquids and coexisting augites, *Contrib. Mineral. Petrol.*, *112*, 196–202, 1992.

[139] *Thy, P., and G. E. Lofgren, Experimental constraints on the low-pressure evolution of transitional and mildly alkalic basalts: The effect of Fe-Ti oxide minerals and the origin of basaltic andesites, *Contrib. Mineral. Petrol.*, *116*, 340–351, 1994.

[140] *Thy, P., G. E. Lofgren, and P. Imsland, Melting relations and the evolution of the Jan Mayen magma system, *J. Petrol.*, *32*, 303–332, 1991.

[141] *Toplis, M. J., and M. R. Carroll, An experimental study of the influence of oxygen fugacity on Fe-Ti oxide stability, phase relations, and mineral-melt equilibria in ferro-basaltic systems, *J. Petrol.*, *36*, 1137–1170, 1995.

[142] *Toplis, M. J., G. Libourel, and R. Carroll, The role of phosphorus in crystallization processes of basalt: An experimental study, *Geochim. Cosmochim. Acta*, *58*, 797–810, 1994.

[143] Tormey, D. R., T. L. Grove, and W. B. Bryan, Experimental petrology of normal MORB near the Kane Fracture Zone: 22°–25° N, mid-Atlantic ridge, *Contrib. Mineral. Petrol.*, *96*, 121–139, 1987.

[144] Treiman, A. H., An alternate hypothesis for the origin of Angra dos Reis: porphyry, not cumulate, *Proc. Lunar Planet. Sci. Conf.*, *9th,* 443–450, 1989.

[145] Ussler, W. I., and A. F. Glazner, Phase equilibria along a basalt-rhyolite mixing line: Implications for the origin of calc-alkaline intermediate magma, *Contrib. Mineral. Petrol.*, *101*, 232–244, 1989.

[146] *Wagner, T. P., J. M. Donnelly-Nolan, and T. L. Grove, Evidence of hydrous differentiation and crystal accumulation in the low-MgO, high-Al2O3 Lake Basalt from Medicine Lake volcano, California, *Contrib. Mineral. Petrol.*, *121*, 201–216, 1995.

[147] *Wagner, T. P., and T. L. Grove, Experimental constraints on the origin of lunar high-Ti ultramafic glasses, *Geochim. Cosmochim. Acta*, *61*, 1315–1327, 1997.

[148] Walker, D., T. L. Grove, J. Longhi, E. M. Stolper, and J. F. Hays, Origin of lunar feldspathic rocks, *Earth Planet. Sci. Lett.*, *20*, 325–336, 1973.

[149] Walker, D., T. Shibata, and S. E. DeLong, Abyssal tholeiites from the Oceanographer fracture zone. I. Phase equilibrium and mixing, *Contrib. Mineral. Petrol.*, *70*, 111–125, 1979.

[150] *Walter, M. J., Melting of garnet peridotite and the origin of komatiite and depleted lithosphere, *J. Petrol.*, *39*, 29–60, 1998.

[151] *Yang, H.-J., R. J. Kinzler, and T. L. Grove, Experiments and models of anhydrous, basaltic olivine-plagioclase-augite saturated melts from.0.001 to 10 kbar, *Contrib. Mineral. Petrol.*, *124*, 1–18, 1996.

Appendix B. Calculation of End-Member Liquid and Solid Gibbs Free Energies at Elevated Temperature and Pressure

[152] The molar Gibbs free energy (standard state chemical potential) of end-member solids at elevated temperature and pressure is calculated by integration along a path comprising a constant pressure and constant temperature segment. Apparent molar enthalpy,

$$\Delta H_{\mathrm{sol},T,P_r} = \Delta H_{f,T_r,P_r} + \int_{T_r}^{T} C_{P,\mathrm{sol}}\,dT + \Delta H_{t,T,P_r},$$

where

$$\Delta H_{t,T,P_r} = \begin{cases} \int_{T_r}^{T} C_{P,\lambda}\,dT & T < T_t \\ \Delta H_t + \int_{T_r}^{T_t} C_{P,\lambda}\,dT & T > T_t \end{cases}$$

and entropy,

$$S_{\mathrm{sol},T,P_r} = S_{T_r,P_r} + \int_{T_r}^{T} \frac{C_{P,\mathrm{sol}}}{T}\,dT + \Delta S_{t,T,P_r},$$

where

$$\Delta S_{t,T,P_r} = \begin{cases} \int_{T_r}^{T} \frac{C_{P,\lambda}}{T}\,dT & T < T_t \\ \frac{\Delta H_t}{T_t} + \int_{T_r}^{T_t} \frac{C_{P,\lambda}}{T}\,dT & T \geq T_t \end{cases}$$

are obtained along the reference isobar and combined with the pressure-integral of the solid equation of state:

$$\Delta G_{\mathrm{sol},T,P} = \Delta H_{\mathrm{sol},T,P_r} - T S_{\mathrm{sol},T,P_r} + \int_{P_r}^{P} V_{\mathrm{sol}}\,dP.$$

Appropriate thermodynamic constants for the relevant solids utilized in pMELTS are taken directly from the MELTS database [see *Ghiorso and Sack*, 1995, Appendix].

[153] The molar Gibbs free energy of end-member liquids is obtained by calculating the molar enthalpy and entropy of the corresponding solid of the same stoichiometry up to the fusion temperature at the reference pressure. To these values we apply the enthalpy and entropy of fusion ($\Delta H_{\mathrm{fus}} = T_{\mathrm{fus}}\Delta S_{\mathrm{fus}}$ and ΔS_{fus}, respectively) to obtain the molar enthalpy and molar entropy of the corresponding liquid. We complete the integration from the fusion temperature to the final temperature by employing the liquid heat capacity. The combined

Table B1. Enthalpy, Entropy, and Heat Capacity Coefficients[a]

Component	$\Delta H_{f,T_r,P_r}$	S_{T_r,P_r}	c_0	$c_1 \times 10^{-2}$	$c_2 \times 10^{-5}$	$c_3 \times 10^{-7}$
Si_4O_8	−3555755	229.696	334.04	−14.988	−98.216	112.028
TiO_2	−961691	50.460	77.84	0	−33.678	40.294
Al_4O_6	−3307937	76.474	310.04	−16.568	−77.228	81.816
Fe_2O_3	−658347	112.813	146.86	0	−55.768	52.563
$MgCr_2O_4$	−1776401	106.02	201.981	−5.519	−57.844	57.729
Fe_2SiO_4	−1465621	157.354	248.93	−19.239	0	−13.910
$MnSi_{1/2}O_2$	−866000	77.950	109.95	−6.355	−10.248	8.826
Mg_2SiO_4	−2166508	106.787	238.64	−20.013	0	−11.624
$NiSi_{1/2}O_2$	−697650	64.050	107.499	−5.1538	−24.723	31.188
$CoSi_{1/2}O_2$	−707050	71.300	100.524	−0.185	−35.905	45.025
$Ca_2Si_2O_6$	−3276717	168.292	282.32	−8.344	−117.152	188.148
$NaSi_{1/2}O_{3/2}$	−800742	56.923	117.39	−11.095	0	6.765
$KAlSiO_4$	−2127829	126.654	186.0	0	−131.067	213.893
$Ca_3(PO_4)_2$	−4083972	235.978	402.997	−28.0835	0	−32.6230
H_2O	664	9.219				

[a] $T_r = 298.15$ K, $P_r = 10^5$ Pa, $\Delta H_{f,T_r,P_r}$: J/mol, S_{T_r,P_r} : J/K-mol, $C_{P,\mathrm{sol}} = c_0 + \frac{c_1}{\sqrt{T}} + \frac{c_2}{T^2} + \frac{c_3}{T^3}$: J/K-mol.

Table B2. Properties Related to Second Order Phase Transitions of Reference Solids[a]

Component	T_t	ΔH_t	$l_1 \times 10^2$	$l_2 \times 10^5$
Fe_2O_3	955	1287	−7.403	27.921
$KAlSiO_4$	800	1154	−7.096	21.682
$Ca_3(PO_4)_2$	1373	14059	2.543	19.255

[a] T_t: K, ΔH_t : J/mol, $C_{P,\lambda} = T(l_1 + l_2 T)^2$:J/K-mol.

result yields the molar Gibbs free energy of the liquid end-member at the reference pressure:

$$\Delta G_{\mathrm{liq},T,P_r} = \Delta H_{\mathrm{sol},T_{\mathrm{fus}},P_r} + T_{\mathrm{fus}}\Delta S_{\mathrm{fus}} + \int_{T_r}^{T} C_{P,\mathrm{liq}}\,dT - T \cdot\left(S_{\mathrm{sol},T_{\mathrm{fus}},P_r} + \int_{T_r}^{T} \frac{C_{P,\mathrm{liq}}}{T}\,dT\right).$$

Values of the constants required to perform this computation are provided in Table B1.

[154] The molar Gibbs free energy of liquid end-member components at elevated pressure is obtained from

$$\Delta G_{\mathrm{liq},T,P} = \Delta G_{\mathrm{liq},T,P_r} + \int_{P_r}^{P} V_{\mathrm{liq}}\,dP. \qquad \text{(B1)}$$

For the liquid, the chosen equation of state is the third-order Birch-Murnaghan equation,

$$P = \frac{3}{2}K\left[\left(\frac{V_0}{V_{\mathrm{liq}}}\right)^{7/3} - \left(\frac{V_0}{V_{\mathrm{liq}}}\right)^{5/3}\right] \cdot\left\{1 - \frac{3}{4}(4 - K')\left[\left(\frac{V_0}{V_{\mathrm{liq}}}\right)^{2/3} - 1\right]\right\}, \qquad \text{(B1)}$$

where V_0 and K are taken to be the volume and bulk modulus, respectively, at T and the reference pressure

$$V_0 = V_{T_r,P_r} + \left.\frac{\partial V}{\partial T}\right|_{T_r,P_r}(T - T_r),$$

$$K = -\frac{V_0}{\left.\frac{\partial V}{\partial P}\right|_{T_r,P_r} + \left.\frac{\partial^2 V}{\partial T \partial P}\right|_{T_r,P_r}(T - T_r)},$$

and K' is taken to be 5 for anhydrous melts (see text; K' for the H_2O component is taken at 3.5). Appropriate values for the required liquid volumetric properties are provided in Table B1.

[155] The integral in equation (A1) is easily evaluated following a method suggested by Asimow

Table B3. Volume and Thermoelastic Coefficients[a]

Component	$V_{T_r,P_r} \times 10^5$	$\left.\frac{\partial V}{\partial P}\right\|_{T_r,P_r} \times 10^9$	$\left.\frac{\partial V}{\partial P}\right\|_{T_r,P_r} \times 10^{15}$	$\left.\frac{\partial^2 V}{\partial T \partial P}\right\|_{T_r,P_r} \times 10^{18}$	T_{fus}	ΔS_{fus}	$C_{P,\mathrm{liq}}$
Si_4O_8	10.760	0.0	−7.56	5.2	1999	17.84	330.4
TiO_2	2.316	7.246	−2.31	0.0	1870	35.82	109.2
Al_4O_6	7.422	5.24	−4.52	5.4	2320	97.22	340.6
Fe_2O_3	4.213	9.09	−2.53	3.1	1895	60.41	240.9
$MgCr_2O_4$	5.358	11.71	−2.26	1.8	2673	73.22	335.1
Fe_2SiO_4	5.420	5.84	−2.79	−2.3	1490	59.9	240.2
$MnSi_{1/2}O_2$	2.84	2.92	−1.40	−1.15	1620	27.6	121.6
Mg_2SiO_4	4.980	5.24	−1.35	−1.3	2163	57.2	271.0
$NiSi_{1/2}O_2$	2.48	2.92	−1.40	−1.15	1923	29.0	119.3
$CoSi_{1/2}O_2$	2.30	2.92	−1.40	−1.15	1688	29.0	125.3
$Ca_2Si_2O_6$	8.694	5.84	−3.10	−3.2	1817	63.0	344.8
$NaSi_{1/2}O_{3/2}$	2.784	3.71	−2.15	−2.65	1361	19.17	90.1
$KAlSiO_4$	6.8375	7.265	−6.40	−4.6	2023	24.5	217
$Ca_3(PO_4)_2$	10.7382		0.0	0.0	1943	35.69	575
H_2O	2.775	10.86	−6.00				

[a] T_r = 1673 K, $P_r = 10^5$ Pa, V_{T_r,P_r} : J/mol, $\left.\frac{\partial V}{\partial T}\right|_{T_r,P_r}$: J/K-Pa-mol, $\left.\frac{\partial V}{\partial P}\right|_{T_r,P_r}$: J/Pa^2-mol, $\left.\frac{\partial^2 V}{\partial T \partial P}\right|_{T_r,P_r}$:J/K-Pa^2-mol, T_{fus} : K, ΔS_{fus} : J/K-mol, $C_{P,\mathrm{liq}}$: J/K-mol.

(P. Asimow, personal communication, 2000). First we define

$$f = \frac{1}{2}\left[\left(\frac{V_0}{V_{\rm liq}}\right)^{2/3} - 1\right] \tag{B3}$$

from which equation (B1) reduces to

$$P = 3Kf(2f+1)^{5/2}\left[1 - \frac{3}{2}f(4-K')\right].$$

Next we rewrite the pressure integral in equation (B1) utilizing integration-by-parts:

$$\int_{P_r}^{P} V_{\rm liq}dP = PV_{\rm liq} - P_rV_0 - \int_{V_0}^{V_{\rm liq}} PdV$$

and change the independent variable of integration from V to f utilizing the definition in equation (B3):

$$\int_{P_r}^{P} V_{\rm liq}dP = PV_{\rm liq} - P_rV_0 - \int_{0}^{f} Pdf. \tag{B4}$$

The integral in equation (B4) can be evaluated analytically:

$$\int_{P_r}^{P} V_{\rm liq}dP = PV_{\rm liq} - P_rV_0 + \frac{9}{2}KV_0f^2[1 + f(K'-4)]. \tag{B5}$$

Combining equations (B1), (B3), and (B5) gives the desired result:

$$\begin{aligned}\Delta G_{{\rm liq},T,P} = {} & \Delta G_{{\rm liq},T,P_r} + PV_{\rm liq} - P_rV_0 \\ & + \frac{9}{8}KV_0\left[\left(\frac{V_0}{V_{\rm liq}}\right)^{2/3} - 1\right]^2 \\ & \times\left\{1 + \frac{1}{2}(K'-4)\left[\left(\frac{V_0}{V_{\rm liq}}\right)^{2/3} - 1\right]\right\}.\end{aligned}$$

All derived thermodynamic properties can be obtained via appropriate temperature and pressure derivatives of this expression.

Acknowledgments

[156] We thank Richard Sack, Ian Carmichael, Becky Lange, Paul Asimow, Peter Kelemen, Mike Baker, and Ed Stolper for their many years of collaborative support, stimulation, feedback, and constructive criticism on the quixotic endeavors of MELTS and thermodynamic calculation of mantle melting. We also gratefully acknowledge the generous support of NSF OCE 9529790 and 9977416 (MSG) and OCE 9711735 and OCE 9977690 (MMH).

References

Agee, C. B., Isothermal compression of molten Fe_2SiO_4, *Geophys. Res. Lett.*, *19*, 1169–1172, 1992a.

Agee, C. B., Thermal expansion of molten Fe_2SiO_4 at high pressure, *Geophys. Res. Lett.*, *19*, 1173–1176, 1992b.

Agee, C. B., and D. Walker, Static compression and olivine flotation in ultrabasic silicate liquid, *J. Geophys. Res.*, *93*, 3437–3449, 1988.

Agee, C. B., and D. Walker, Aluminum partitioning between olivine and ultrabasic silicate liquid to 6 GPa, *Contrib. Mineral. Petrol.*, *105*, 243–254, 1990.

Agee, C. B., and D. Walker, Olivine flotation in mantle melt, *Earth Planet. Sci. Lett.*, *114*, 315–324, 1993.

Asimow, P. D., and E. M. Stolper, Steady-state mantle-melt interactions in one dimension, I, Equilibrium transport and melt focusing, *J. Petrol.*, *40*, 475–494, 1999.

Asimow, P. D., M. M. Hirschmann, M. S. Ghiorso, M. J. O'Hara, and E. M. Stolper, The effect of pressure-induced solid-solid phase transitions on decompression melting of the mantle, *Geochim. Cosmochim. Acta*, *59*, 4489–4506, 1995.

Asimow, P. D., M. M. Hirschmann, and E. M. Stolper, An analysis of variations in isentropic melt productivity, *Philos. Trans. R. Soc. London Ser. A*, *355*, 255–281, 1997.

Asimow, P. D., M. M. Hirschmann, and E. M. Stolper, Calculation of peridotite partial melting from thermodynamic models of minerals and melts, IV, Adiabatic decompression and the composition and mean properties of mid-ocean ridge basalts, *J. Petrol.*, *42*, 963–998, 2001.

Baker, M. B., and E. M. Stolper, Determining the composition of high-pressure mantle melts using diamond aggregates, *Geochim. Cosmochim. Acta*, *58*, 2811–2827, 1994.

Baker, M. B., M. M. Hirschmann, M. S. Ghiorso, and E. M. Stolper, Compositions of near-solidus peridotite melts from experiments and thermodynamic calculation, *Nature*, *375*, 308–311, 1995.

Barron, L. M., The calculated geometry of silicate liquid immiscibility, *Geochim. Cosmochim. Acta*, *45*, 495–512, 1981.

Berman, R. G., Internally-consistent thermodynamic data for minerals in the system Na_2O-K_2O-CaO-MgO-FeO-Fe_2O_3-Al_2O_3-SiO_2-TiO_2-H_2O-CO_2, *J. Petrol.*, *29*, 445–522, 1988.

Burnham, C. W., J. R. Holloway, and N. F. Davis, *Thermodynamic Properties of Water to 1000°C and 10000 Bars*, 96 pp., Geol. Soc. of Am., Boulder, Colo., 1969.

Circone, S., and C. B. Agee, Compressibility of molten high-Ti mare glass; evidence for crystal-liquid density inversions in the lunar mantle, *Geochim. Cosmochim. Acta*, *60*, 2709–2720, 1996.

Eiler, J. M., A. J. Crawford, T. R. Elliott, K. A. Farley, J. W. Valley, and E. M. Stolper, Oxygen isotope geochemistry of oceanic-arc lavas, *J. Petrol.*, *41*, 229–256, 2000.

Falloon, T. J., D. H. Green, L. V. Danyushevsky, and U. H. Faul, Peridotite melting at 1.0 and 1.5 GPa: An experi-

mental evaluation of techniques using diamond aggregates and mineral mixes for determination of near-solidus melts, *J. Petrol.*, *40*, 1343–1375, 1999.

Gaetani, G. A., and T. L. Grove, The influence of water on melting of mantle peridotite, *Contrib. Mineral. Petrol.*, *131*, 323–346, 1998.

Ghiorso, M. S., LSEQIEQ: A FORTRAN IV subroutine package for the analysis of multiple linear regression problems with possibly deficient pseudorank and linear equality and inequality constraints, *Comput. Geosci.*, *9*, 391–416, 1983.

Ghiorso, M. S., Thermodynamic models of igneous processes, *Ann. Rev. Earth Planet. Sci.*, *25*, 221–241, 1997.

Ghiorso, M. S., and I. S. E. Carmichael, A regular solution model for met-aluminous silicate liquids; applications to geothermometry, immiscibility, and the source regions of basic magmas, *Contrib. Mineral. Petrol.*, *71*, 323–342, 1980.

Ghiorso, M. S., and R. O. Sack, Chemical mass transfer in magmatic processes, IV, A revised and internally consistent thermodynamic model for the interpolation and extrapolation of liquid-solid equilibria in magmatic systems at elevated temperatures and pressures, *Contrib. Mineral. Petrol.*, *119*, 197–212, 1995.

Ghiorso, M. S., I. S. E. Carmichael, M. L. Rivers, and R. O. Sack, The Gibbs free energy of mixing of natural silicate liquids: An expanded regular solution approximation for the calculation of magmatic intensive variables, *Contrib. Mineral. Petrol.*, *84*, 107–145, 1983.

Haar, L., J. S. Gallagher, G. S. Kell, *NBS/NRC Steam Tables: Thermodynamic and Transport Properties and Computer Programs for Vapor and Liquid States of Water in SI Units*., 318 pp., Hemisphere, Washington D.C., 1984.

Herzberg, C., and J. Zhang, Melting experiments on komatiite analog compositions at 5 GPa, *Am. Mineral.*, *82*, 354–367, 1997.

Hirschmann, M. M., Mantle solidus: Experimental constraints and the effects of peridotite composition, *Geochem. Geophys. Geosys*., *1*, 2000GC000070, 2000. (Available at http://www.g-cubed.org)

Hirschmann, M. M., and M. S. Ghiorso, Activities of nickel, cobalt, and manganese silicates in magmatic liquids and applications to olivine/liquid and to silicate/metal partitioning, *Geochim. Cosmochim. Acta*, *58*, 4109–4126, 1994.

Hirschmann, M. M., M. B. Baker, and E. M. Stolper, The effect of alkalis on the silica content of mantle-derived melts, *Geochim. Cosmochim. Acta*, *62*, 883–902, 1998a.

Hirschmann, M. M., M. S. Ghiorso, L. E. Wasylenki, P. D. Asimow, and E. M. Stolper, Calculation of peridotite partial melting from thermodynamic models of minerals and melts, I, Review of methods and comparison with experiments, *J. Petrol.*, *39*, 1091–1115, 1998b.

Hirschmann, M. M., P. D. Asimow, M. S. Ghiorso, and E. M. Stolper, Calculation of peridotite partial melting from thermodynamic models of minerals and melts, III, Controls on isobaric melt production and the effect of water on melt production, *J. Petrol.*, *40*, 831–851, 1999a.

Hirschmann, M. M., M. S. Ghiorso, and E. M. Stolper, Calculation of peridotite partial melting from thermodynamic models of minerals and melts, II, Isobaric variations in melts near the solidus and owing to variable source composition, *J. Petrol.*, *40*, 297–313, 1999b.

Holloway, J. R., Graphite-melt equilibria during mantle melting; constraints on CO_2 in MORB magmas and the carbon content of the mantle, *Chem. Geol.*, *147*, 89–97, 1998.

Huebner, J. S., Buffering technique for hydrostatic systems at elevated pressures, in *Research Techniques for High Pressure and High Temperature*, edited by G. C. Ulmer, pp. 123–177, Springer-Verlag, New York, 1971.

Kelemen, P. B., and H. J. B. Dick, Focused melt flow and localized deformation in the upper mantle: Juxtaposition of replacive dunite and ductile shear zones in the Josephine Peridotite, SW Oregon, *J. Geophys. Res.*, *100*, 423–438, 1995.

Kress, V. C., and I. S. E. Carmichael, The compressibility of silicate liquids containing Fe_2O_3 and the effect of composition, temperature, oxygen fugacity and pressure on their redox states, *Contrib. Mineral. Petrol.*, *108*, 82–92, 1991.

Kushiro, I., Partial melting of a fertile mantle peridotite at high pressures: An experimental study using aggregates of diamond, in *Earth Processes: Reading the Isotopic Code*, pp. 109–122, 1996.

Kushiro, I., Compositions of partial melts formed in mantle peridotites at high pressures and their relation to those of primitive MORB, *Phys. Earth Planet. Int.*, *107*, 103–110, 1998.

Kushiro, I., Partial melting experiments on peridotite and origin of mid- ocean ridge basalt, *Ann. Rev. Earth Planet. Sci.*, *29*, 71–107, 2001.

Lange, R. L., and I. S. E. Carmichael, Thermodynamic properties of silicate liquids with emphasis on density, thermal expansion and compressibility, in *Modern Methods Of Igneous Petrology: Understanding Magmatic Processes*, vol. 24, pp. 25–64, Mineral. Soc. of Am., Washington, D.C., 1990.

Lawson, C. L., and R. J. Hanson, *Solving Least Squares Problems*, 340 pp., Prentice Hall, New Jersey, 1974.

Longhi, J., The anhydrous mantle solidus? New experiments in CMAS, *EOS Trans. AGU*, *79*(46), Fall Meet. Suppl.,F1005, 1998.

Luth, R. W., Measurement and control of intensive parameters in experiments at high pressure in solid-media apparatus, in *Experiments at High Pressure and Applications to the Earth's Mantle*, vol. 21, edited by R.W. Luth, pp. 15–38, Mineral. Assoc. of Can., Edmonton, 1993.

Miller, G. H., E. M. Stolper, and T. J. Ahrens, The equation of state of a molten komatiite, 1, Shock wave compression to 36 GPa, *J. Geophys. Res.*, *96*, 11,831–11,848, 1991.

Ochs, F. A., III, and R. L. Lange, The partial molar volume, thermal expansivity, and compressibility of H_2O in $NaAlSi_3O_8$ liquid: New measurements and an internally consistent model, *Contrib. Mineral. Petrol.*, *129*, 155–165, 1997.

Pickering-Witter, J., and A. D. Johnston, The effects of variable bulk composition on the melting systematics of fertile peridotitic assemblages, *Contrib. Mineral. Petrol.*, *140*, 190–211, 2000.

Pitzer, K. S., and S. M. Sterner, Equations of state valid continuously from zero to extreme pressures for H_2O and CO_2, *J. Chem. Phys.*, *101*, 3111–3116, 1994.

Press, W. H., P. Flannery, S. Teukolsky, and W. Vetterling, *Numerical Recipes in C*, 1020 pp., Cambridge Univ. Press, New York, 1992.

Rigden, S. M., T. Ahrens, and E. M. Stolper, High-pressure equation of state of molten anorthite and diopside, *J. Geophys. Res.*, *94*, 9508–9522, 1989.

Robinson, J. A. C., B. J. Wood, and J. D. Blundy, The beginning of melting of fertile and depleted peridotite at 1.5 GPa, *Earth Planet. Sci. Lett.*, *155*, 97–111, 1998.

Sack, R. O., and M. S. Ghiorso, Thermodynamics of multicomponent pyroxenes, I, Formulation of a general model, *Contrib. Mineral. Petrol.*, *116*, 277–286, 1994.

Schiano, P., J. M. Eiler, I. D. Hutcheon, and E. M. Stolper, Primitive CaO-rich, silica-undersaturated melts in island arcs: Evidence for the involvement of clinopyroxene-rich lithologies in the petrogenesis of arc magmas, *Geochem. Geophys. Geosys.*, *1*, 1999GC000032, 2000. (Available at http://www.g-cubed.org)

Schwab, B., and A. D. Johnston, Melting systematics of modally variable, compositionally intermediate peridotites and the effects of mineral fertility, *J. Petrol.*, *42*, 1789–1811, 2001.

Walter, M. J., Melting of garnet peridotite and the origin of komatiite and depleted lithosphere, *J. Petrol.*, *39*, 29–60, 1998.

Walter, M. J., Y. Thibault, E. Wei, and R. W. Luth, Characterizing experimental pressure and temperature conditions in multi-anvil apparatus, *Can. J. Phys.*, *73*, 273–286, 1995.